Egyptian Journal of Geology, v. 63, 2019, p. 267-290

MINERALOGICAL AND GEOCHEMICAL CHARACTERISTICS OF EL-MISSIKAT FLUORITE MINERALIZATION, CENTRAL EASTERN DESERT, EGYPT: TRACE ELEMENTS AND FLUID INCLUSIONS CONSTRAINTS

Bottros R. Bakhit

Geology Department, Faculty of Science, Beni-Suef University, Beni-Suef, Egypt
E-mail: drbottros@yahoo.com and drbottros@science.bsu.edu.eg

ABSTRACT

Fluorite of different colours occurs as disseminations and veinlets in the host granitic rocks in El-Missikat area, central Eastern Desert, Egypt. This paper addresses the mineralogical and geochemical characteristics, including mineral chemistry, whole rock geochemical analyses of the granitic host rock. Trace, REY (REE+Y) elements, fluid inclusions and LA-ICP-MS analyses for individual fluid inclusions in fluorite were also carried out. Petrographically, the host granite represented by biotite granite. Mineral chemistry data of primary phases are given. Plagioclase is albite (average 2.79 mol%). Biotite is of primary magmatic origin and crystallized at 500 - 600^{o}C. Geochemically, El-Missikat granite is peraluminous A- type and was generated in post-collision environment (within plate).

The average ΣREE content of Type V (violet), G (green) and Type W (white) fluorite samples are 75.5, 200.9 and 203.2 ppm, respectively (i.e. increasing from violet fluorite to green and white fluorites. These differences in ΣREE were possibly related to changes in pH condition and bulk chemical composition of the fluids. Tb/Ca, Tb/La and Y/Ho ratios of the fluorite types indicate that they were formed from the interaction between magmatic fluids and granitic wall-rocks. The fluorites show strongly negative Eu and positive Y anomalies similar to REY pattern of the host granites, indicating that the source of REE and trace elements of hydrothermal fluids is the host granite leached by fluids. The present work revealed that the contents of Y and total REE contents are responsible for the appearance of green and white colours. The Sr content is high in violet fluorite and may be responsible for violet colour.

The fluid inclusions (FI) of the fluorite have homogenisation temperatures ranging from 201^{o}C to 296^{o}C in Type A (high salinity FI) and 160^{o}C to 165^{o}C in Type B **(**low salinity FI). The melting temperature of ice in fluorite indicates salinities up to 19.4 equiv. wt% Na CI (Type A) but Type B FI have a low range of salinity (0.53 to 4.49 equiv. wt% Na Cl). The density of fluids is 0.9 to 1.0 g/cm^{3} in Type A and 0.9 g/cm^{3} in Type B. From the LA-ICP-MS data for the individual FI of El-Missikat fluorite, it is clear that the Type A FI contains very high concentrations of elements than that in Type B FI. The abundance of the analyzed elements in the present FI is: Ca > Na > S > K > Sr > Y > Fe, Pb > Cu > U > Cs, W, Te, Ag, As > Th > Au. The deposition mechanisms for fluorite may be fluid mixing, changes in pressure and temperature and fluid-rock interaction.

Keywords: Fluorite; Trace elements; Fluid inclusions; El-Missikat Egypt.

INTRODUCTION

Fluorite is widely distributed among the basement rocks of Egypt; it is formed during a late magmatic crystallization of younger (alkaline and per-alkaline) granites as disseminations or as late-crystallization hydrothermal deposits (Sabet et al., 1976 and Hussein, 1990). More than twenty five occurrences of fluorite are known in the Eastern Desert of Egypt (Wassef et al., 1973), they are almost localized in the central and southern parts. Numerous geological and geochemical data on the fluorite veins in the Eastern Desert were carred out (e.g.Yonan,1990; El-Mansi, 1993; Mohamed and Bishara, 1998; Fawzy et al.,1996; Fawzy, 2001; Salem et al., 2001; Ali, 2001; Yonan and El-Kammar, 2001; Mohamed, 2013; Mahdy et al., 2013, El Hadek et al., 2016 and Fawzy, 2017).

The crystal structure of fluorite permits incorporation of many genetically important trace and rare-earth elements (Möller et al., 1998). The similar ionic radius rare-earth elements allow them to substitute for Ca in fluorite. The amount of trace elements incorporated into fluorides largely depends on their availability in the melt fluid. Therefore, REE patterns and trace element contents could reflect the source (i.e., fluid or melt) from which they crystallized or precipitated (Sallet et al., 2000), and REE in fluorites are often used to trace the REE content of an associated hydrothermal fluid (Hill et al., 2000).

Fluid inclusions in minerals are tiny blebs of fluid, that found trapped within single crystals. They are considered the direct evidence for the pressure, temperature, density and composition of the mineral-forming fluids. Their study provides important tools for understanding the genesis of hydrothermal mineral deposits (Roedder, 1984; Roedder and Bodnar, 1997; Robb, 2005; Pirajno, 2009).

Geology of the El-Missikat area has been dealt with many authors (e.g. Bakhit, 1978; Hussein et al., 1986; Mohamed, 1995; Abu Dief et al., 1997; El-Mansi, 2000 and Raslan, 2008 & 2009). They reported that, the uranium mineralization (mainly uranophane) in El-Missikat occurrence is associated with jasperoid veins found along the faults and fractures that are mainly filled with silica in typical shear zones. Visible deep-blue to violet fluorite crystals were recorded in other parts of El-Missikat, highly sheared mineralized granite that are very strongly radioactive, but without any visible uranium mineralization.

GEOLOGIC SETTING

El-Missikat area is located in the central part of the Eastern Desert of Egypt, midway between Safaga on the Red Sea coast and Qena in the Nile Valley, at about 85 km. from each. The present area is covered by younger granites and metamorphosed volcano-sedimentary rocks (Fig. 1).

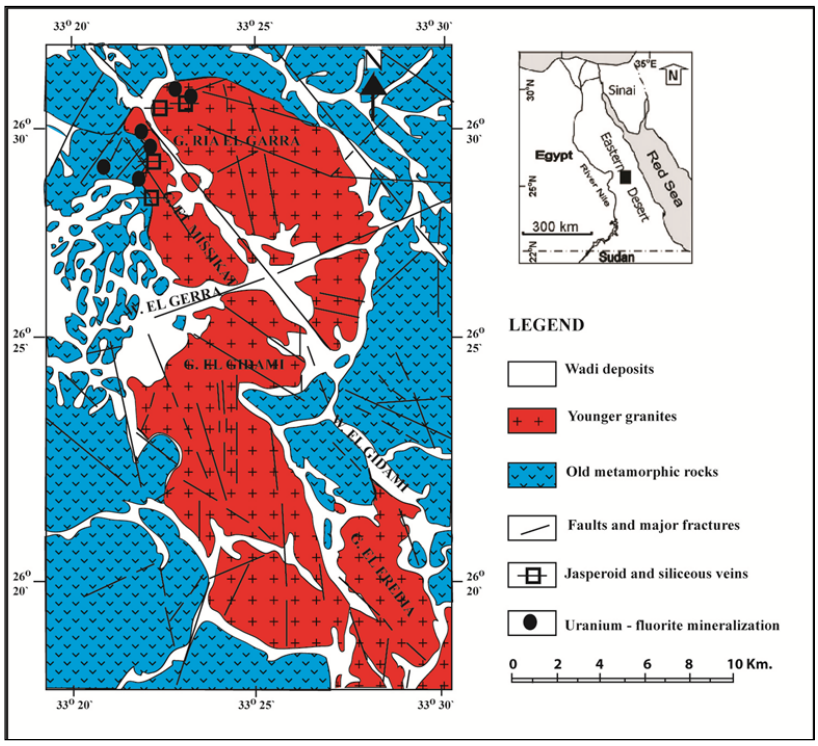

Fig. 1. Geological map of El-Missikat area (after Bakhit and El Kassas, 1989).

The younger granites occur as highly elevated lensoidal mass intruding the metabasalts and meta-sedimentary sequence cropping out in the area with sharp contacts. They are medium to coarse-grained with light pink color. They possess exfoliation, cavernous appearance and well pronounced subvertical jointing. The present granites are intersected by sets of faults trending approximately N, NW and EW.

El-Missikat granite is transected by several jasperoid, siliceous veins and fluorite veins (Fig. 1). They represent fissure fillings developed mainly along the fault planes. Fluorite forms intersected veinlets

forming stockwork up to 2 m width as well as disseminated crystals in the wall zone (Fig. 2a). An alteration zone associating the main fluorite vein is represented by very friable highly altered greenish white kaolinitic rock (Fig. 2b). The alteration gradually weaken away from the vein passing to slightly altered granite still preserving its original texture. The most characteristic alteration processes affecting the El-Missikat younger granites are kaolinization and sericitization. The fluorite forms coarse-grained cubic crystals and display a range of colours including green, violet and white (Fig. 2c).

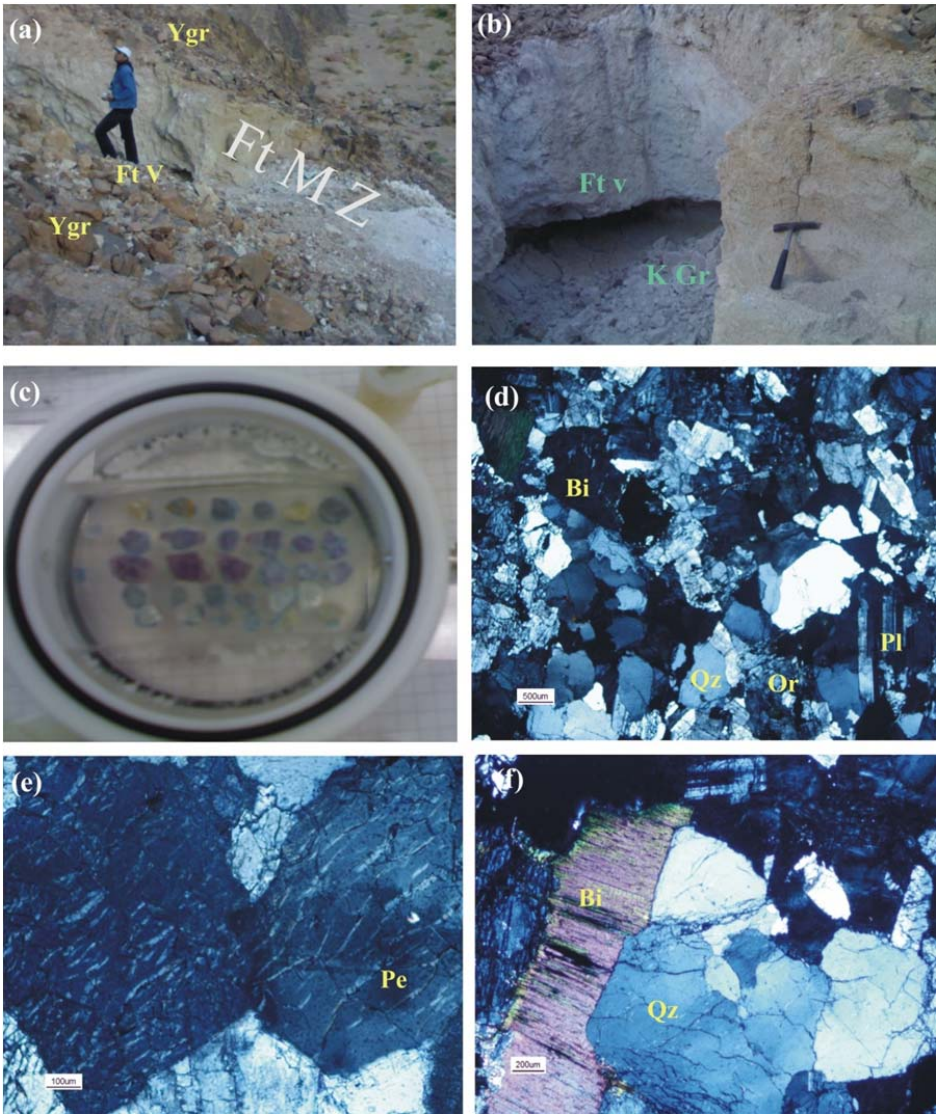

Fig. 2: Characteristics of El-Missikat granite. (a) Fluorite mineralized zone (Ft MZ) developed along shear zone in El-Missikat younger granite (YGR) Note the worked out fluorite veins (FtV); (b) Fluorite veinlets (Ft v) along shaft in highly altered kaolinized granites (KGr); (c) Different colors of fluorite from the main mineralized zone prepared to ICP-MS analyses; (d) Coarse-grained allotriomorphic texture of biotite granite composed of quartz (Qz), feldspars (Or and pl) and biotite (Bi), C.N.; (e) Perthitic texture in El Missikat granite C.N.; (f) Biotite (Bi) slightly corroded by quartz (Qz) in El-Missikat biotite granite C.N.

ANALYTICAL TECHNIQUES

Primary minerals were analyzed using a JEOL JXA-8200 electron probe microanalyzer equipped with five wavelength dispersive spectrometers (WDS). The mineral analyses were made with a counting time of 20 s, an accelerating voltage of 15 kV and a beam current of 20 nA.

Major element compositions were determined using a wave-length dispersive X-ray fluorescence spectrometer (WD-XRF, Axios, PANalytical), equipped with 5 diffraction crystals, using fusion glasses made from a mixture powdered sample and lithium-tetraborate ($Li_2B_4O_7$) in the proportion 1:5. Calibration was based on ca. 30 certified international standards. Trace and rare earth elements were analyzed using laser ablation inductively coupled plasma mass spectrometry (LA-ICP-MS), using the same fused pellets prepared for the major elements determination. The laser ablation system is an ArF (argonfluorin) eximer laser at 193 nm with a prototype beam delivery system similar to the Geolas system. The dry aerosol from laser ablation was measured with a Perkin Elmer Elan 6100 DRC quadrupole ICP-MS. Three spots were analyzed for each pellet (sample), and then the average was calculated. Each ablation was carried out for a period of 60 s. Laser ablation parameters were: spot diameter=90 μm, frequency=10 Hz, energy density ~20 J/cm2, helium as ablation medium. The glass reference material SRM 610 from NIST was used as calibration standard. The ability of LA-ICP-MS method to determine accurately and precisely trace elements (including key elements such as REE, Nb, Ta, Zr, etc.) in bulk geological samples is well documented (e.g. Eggins, 2003; Jochum et al., 2005). The details of geochemical and mineral chemical analyses are given in Basta et al. (2011 & 2017).

Microthermometric measurements were conducted on fluorite double polished samples, less than 500 μm thick, using a Linkam THMSG-600 heating-freezing stage. All measurements were performed twice, to test the precision of the data with a heating rate of 0.1^{o}C, except for the total homogenization temperature. They were measured with a heating rate of 1^{o}C. Calibration was performed on synthetic fluid inclusion standards by SYN FLINC to ± 0.1 ^{o}C at the melting points of CO_2 (-56.6 ^{o}C) and H_2O (0.0 ^{o}C), and to ± 1 ^{o}C at the critical point of pure H_2O (374.1 ^{o}C). Apparent salinities of the natural fluid inclusions are reported in wt. % NaCl (eq.), bases on final melting of ice (Bodnar and Vityk, 1994). This salinity estimate is needed as an internal standard for LA-ICP-MS. The total homogenization temperature was commonly measured after ICP-MS chemical analysis using remaining fluid inclusions on the same assemblages.

Laser-Ablation-ICP-MS measurements were performed with a Perkin Elmer Elan 6100 DRC quadrupole ICP mass spectrometer, with which it is possible to simultaneously quantify selected elements in single fluid inclusions using a beam homogenized 193 nm excimer laser ablation system (Geolas, ETH prototype). With this instrumentation the analytical error due to element fractionation is reduced to the typical precision of 2-5% achieved by quadrupole LA-ICP-MS in multi-element (Heinrich et al., 2003). Before and after every series of measurements the standard NIST SRM 610 was measured twice. Data reduction and quantification were done with the computer program SILS (Guillong et al., 2008). More detailed description of the quantification approach for fluid inclusions is given in (1996; Günther et al., 1998; Halter et al., 2002; Heinrich et al., 2003).

All the mineral analyses, whole-rock XRF and ICP-MS analyses as well as the fluid inclusions analyses were performed at the Institute of Geochemistry and Petrology, ETH-Zurich, Switzerland.

CHARACTERIZATION OF THE GRANITIC HOST ROCK

Petrography and opaque mineralogy

El-Missikat granite pluton is represented by biotite-granite. The rock is coarse-grained, allotriomorphic granular, composed of orthoclase, plagioclase, quartz and biotite (Fig**.** 2d). Opaques are accessory. Orthoclase is usually fresh and occurs as very big anhedral grains corroding and engulfing plagioclase. Flame perthite is common **(**Fig**.** 2e), formed of lens-shaped and linear bodies of albite in k-feldspar host. In many cases, the flame perthites coalesce to form flake perthite**.** Sometimes k-feldspars engulf small plagioclase prisms**.** Plagioclase is present as medium subhedral prisms with kaolinized cores and fresh rims. The fresh crystals show lamellar twinning. Quartz occurs as anhedral complex grains occupying the interstitial spaces between feldspars and corroding K-feldspar and plagioclase. Biotite (Fig. 2f) is present as subhedral prisms strongly pleochroic from yellow to black and sometimes altered to chlorite and slightly corroded by quartz. Opaques constitute less than 1 % and are represented by ilmenite and small amount of pyrite. Ilmenite occurs as discrete subhedral prismatic crystals partly to completely altered to titanite or hematite and rutile. Pyrite occurs as small inclusions in ilmenite.

Mineral chemistry

Chemical compositions of the essential rock-forming minerals were determined in the biotite granite of El-Missikat area. The analysed minerals include biotite and feldspars. Electron microprobe analyses were used to classify these minerals and to deduce both magma type and tectonic environments of the studied granites.

Biotite

Representative EMPA analyses of the biotite crystals are given in Table 1. In general, biotite has relatively high concentrations of Al_2O_3 (17.36–19.18 wt %) and FeO(t) (26.9–28.87 wt%), and low contents of MnO (0.79–1.06 wt%) and TiO_2 (1.52–2.33 wt%). On Fe/Fe + Mg vs. Si diagram (Fig. 3a) given by Rieder et al. (1998), the analyzed biotites plot in the biotite field. On a ternary diagram of MgO – FeO(t) - Al_2O_3, Nockolds (1947) and TiO_2–FeO(t)–MgO ternary diagram of Nachit et al. (2005), the analysed biotites are similar to primary igneous biotites (Figs. 3b&c). The composition of igneous biotite can be used to reflect the nature of their host magmas (Abdel-Rahman, 1994; Nachit et al., 1985). On the biotite discrimination diagram of Abdel-Rahman (1994), the analyzed biotites plot in the field of peraluminous granites (Fig. 3d).

The concentration of Ti in biotite is very sensitive to temperature and fO_2, making it possible to use biotite to obtain temperature estimates for igneous and metamorphic rocks (Patino Douce, 1993). Henry et al. (2005) used the binary diagram Ti versus Mg/(MgO+Fe^2) to calculate the crystallization temperatures of biotites. On this diagram (Fig. 3e), the primary biotite yields temperatures around 500 to 600°C.

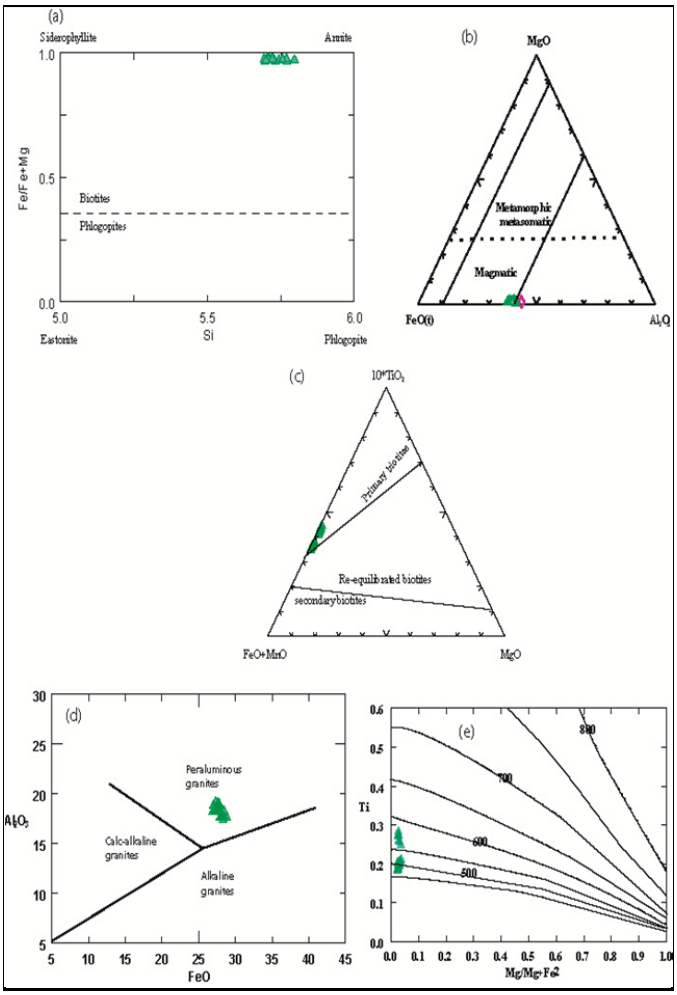

Fig. 3: Characteristics of the biotite in the biotite granite of the area. (a) Si-Fe/(Fe+Mg) diagram after Rieder et al. (1998); (b) FeO(t) - MgO - Al_2O_3 ternary diagram of the studied biotite / / zone demarked by Nockolods (1947) for igneous rocks..... Line drawn by Gokhale (1968) separating biotites of magmatic from these of metamorphic-metasomatic rocks; (c) FeO+MnO-10*TiO_2-MgO ternary diagram after Nachit et al. (2005) and (d) Al_2O_3 vs. FeO(t) diagram after Abdel-Rahman (1994); (e) Mg/(MgO+Fe^2) vs. Ti diagram of biotite with crystallization temperatures after Henry et al. (2005).

Feldspars

The compositions of plagioclase and K-feldspar from the present granite are given (Table_2). The plagioclase of the biotite granite is essentially albite with low An contents (2.79–6.44 mol %). The plagioclase lamellae in the perthite of the biotite granite have the composition of albite (An = 1.06–1.88 mol %). The composition range of orthoclase is An $_{0.02\ to\ 0.42}$, Ab $_{1.56\ to\ 16.17}$, Or $_{83.42\ to\ 98.35}$ mol%.

Geochemical characteristics and classifications

Representative chemical analyses of major, trace and REE abundances of El-Missikat granites are listed in Table 3. The studied granites have high content of SiO_2 (76.31-82.13 wt. %), K_2O (3.2-4.7 wt. %) and Na_2O (0.11-4.2 wt.%) and low content of $Fe_2O_3^t$ (0.55-1.19 Wt.%), MgO (0.01-0.08 Wt.%) and CaO (0.08-0.73 wt.%). Although the CaO content of El-Missikat granite is low, it is still slightly high compared to the same rock type from elsewhere in the CED of Egypt (Eliwa et al., 2014; Farahat et al., 2011), due to the widespread occurrence of late stage phases such as fluorite.

Many classification schemes were applied for the studied granitic rocks. On Total alkalis-silica (TAS) diagram of Middlemost (1991) (Fig. 4a), the present granites fall in the granite field. On K_2O vs. SiO_2 (Fig. 4b), El-Missikat granites are classified as high-K calc-alkaline rocks. According to the criteria of Frost et al. (2001), the studied granites have calcic to alkali-calcic characters (Fig. 4c). The present granites are mostly peraluminous (Fig. 4d). In terms of $FeO^t/(FeO^t + MgO)$ (Frost et al., 2001), the El-Missikat granites completely occupy the ferroan field (Fig. 4e).

The MORB-normalized spider patterns of El-Missikat granites (Fig. 4f) show considerable enrichment in K, Rb and Th and lesser degree of enrichment in HFSE, except Y and Yb which have normalized values slightly higher than N-MORB normalized values. These patterns lack the pronounced Nb and Ta anomalies, which characterize the patterns of gabbros and older granitoids from the Nubian Shield of Egypt (Maurice et al., 2013 and Basta et al., 2017) but they display strongly negative anomalies in Sr, Ba, P and Ti. These negative anomalies can be attributed to the fractionation of feldspars, apatite and Fe-Ti oxides.

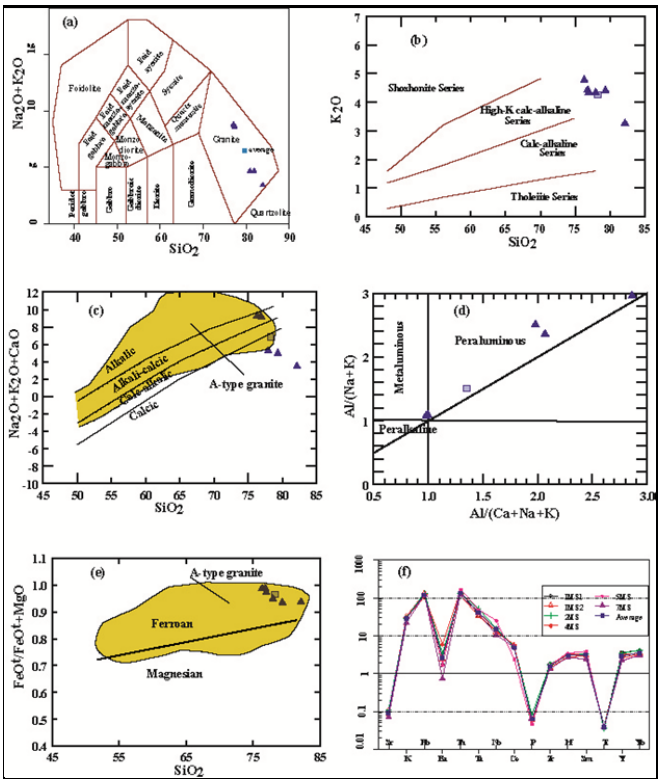

Fig. 4. Chracterization of El-Missikat granitic rocks. (a) SiO_2-Na_2O+K_2O diagram (after Middlemost, 1991); (b) SiO_2 vs K_2O diagram (after Peccerillo and Taylor, 1976); (c) SiO_2-Na_2O+K_2O-CaO diagram (after Frost et al., 2001); (d) A/NK (molar Al_2O_3/Na_2O+ K_2O) vs. A/CNK (molar $Al_2O_3/CaO + Na_2O + K_2O$) (Maniar and Piccoli, 1989); (e) SiO_2 versus FeO^t/FeO^t+ MgO binary diagram showing that granitic rocks are ferroan (Frost et al. 2001) ; (f) MORB-normalized spider diagrams of whole-rock trace-element abundance. MORB normalization values after Pearce (1983).

THE FLUORITE MINERALIZATION

Petrography

Fluorite occurs as coarse massive aggregates. The individual crystals (Fig. 5a) are euhedral to subhedral characterized by high relief, cracking and isotropism. The crystals are up to 5 mm in length, and some show two sets of cleavage. Besides occurring as interstitial grains between the perthite, quartz and opaques (Fig. 5b), the fluorite crystals are generally found as filling microfractures and cavities in the highly sheared granite, which reflects their late origin as a result of the hydrothermal alteration of the granites. Fluorite crystals are corroded by quartz and invaded by thin calcite veinlets.

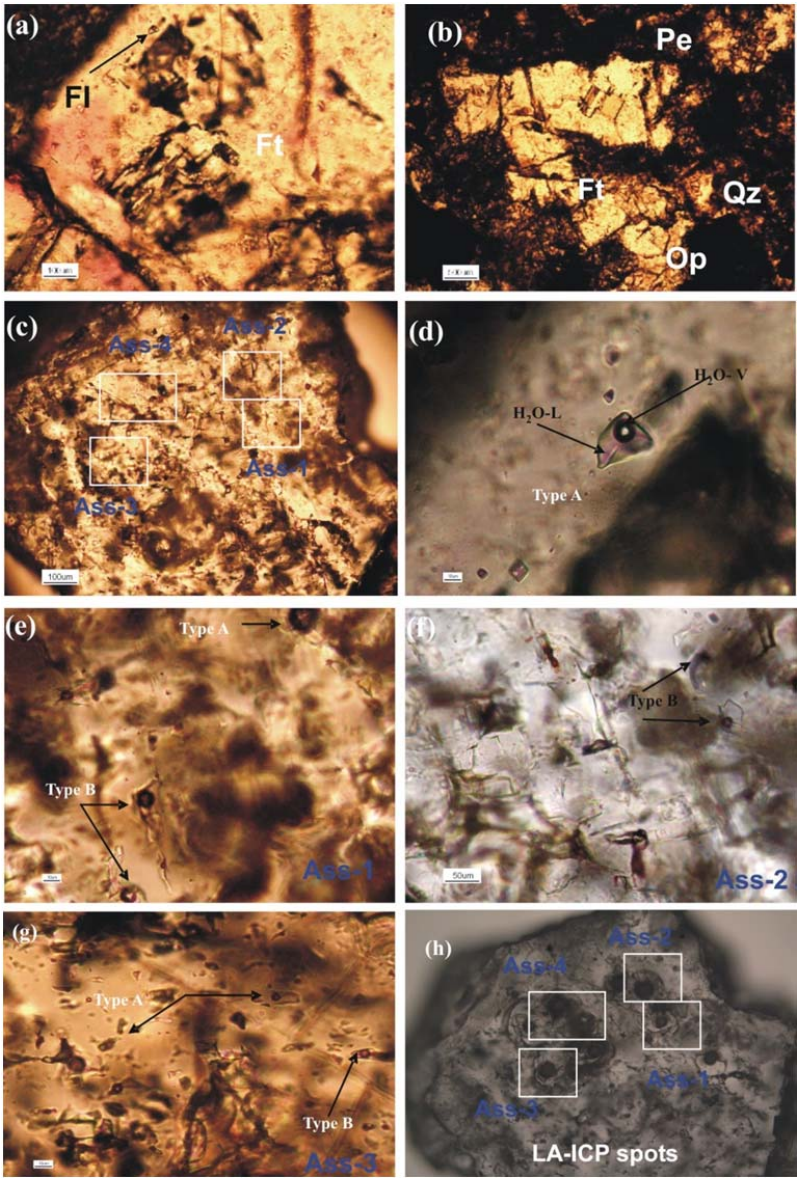

Fig. 5: Characterization of El-Missikat fluorite. (a) Euhedral fluorite crystal (Ft) showing high relief and cracking. Note the fluid inclusion (FI) along the growth zone. ppl; (b) Fluorite (Ft) occupying the interstitial space between quartz (Qz), perthite (pe) and opaque (Op). P.L.; (c) Photograph of the different fluid inclusion assemblages (Ass-1 to 4) occurring within the green Missikat florite. PL; (d) Primary FI (high salinity aqueous fluids; type A) developed along the growth zone of fluorite, P.L. ; (e - g) close – up view of photo c showing the different fluid inclusion assemblages contain only two types of FI (Type A; high salinity FI and Type B, low salinity FI. P.L.; (h) Distribution of LA-ICP-MS analyses spots in different FI assemblages (Ass-1 to 4) P.L.

Trace elements distribution

Trace and REE contents of violet, white and green fluorites from El-Missikat area are listed in Table 4. The trace elements show wide range of variation, particularly Sr (35.4 to 1113.6 ppm), Y (25.1 to 1697.7 ppm), Na (15.6 to 100.1 ppm), K (10.6 to 225 ppm), Co (0.23 to 159.7 ppm), Al (15 to 621 ppm) and REE (33 to 329 ppm) while the other elements have small variation range.

Strontium can be incorporated as cation into fluorite due to their similar size and same charge to Ca. Distribution of Sr indicates that, the violet fluorite varieties have higher Sr contents (average=431.9 ppm) than the white (average=84.3ppm) and green (average= 70.01 ppm) fluorites. The average of Sr content of El-Missikat fluorite samples is higher than that for the hydrothermal worldwide fluorites (56 ppm, Barbieri et al., 1984). Deng et. al, 2014 studied the fluorite in Tumen deposit, China and they found that the Sr content in type 1 (white fluorite) range from 658.8 to 1117 ppm (average 912 ppm) while the type 2a (purple fluorite) have Sr contents between 882 to 1564 with an average of 1137 ppm. The present average of Sr for the violet variety is higher than the worldwide average which may indicate a relation between coloration and Sr concentration in fluorite. Y was detected in all samples of fluorite at concentrations of 25.1 to 1259.7 ppm. Although the ranges of Y contents are rather broad, it can be recognized that the green fluorite has the greater Y content (average=823.7 ppm), whereas the violet fluorites have lower contents of Y (128.5 ppm). The white fluorite have a high content of Y (average = 819.6 ppm). Copper detected only in the violet fluorite, ranges from 1.94 to 3.56 ppm, with an average of 2.75 ppm. U is not detected in the violet variety, but it is recorded in the white (0.3 to 1.96 ppm, average=1.13 ppm) and green (0.69 to 3.90m average=1.65) varieties. The Th content is very low in violet, white and green fluorites (average is 0.2, 1.13 and 1.65 respectively). The mutual distribution of the elements Na, K, Cr, Co, Ni, Fe, Sn, Mn, pb, Zn and Rb is random and reflects no coherence to fluorite coloration.

Fluorite grains from the different colours show different REE content (Table 4). Total REE concentrations (ΣREE) in violet fluorites range from 33.02 to 134.55 ppm (average 75.47 ppm), white fluorite from 129.2to 285.4 ppm (average 203.02 ppm), and green variety from 142.7 to 312 ppm (average 200.95 ppm). From this data, it is clear that white and green fluorites have higher ΣREE values than violet type.

Fluid inclusions

Fluid inclusion assemblages (Goldstein and Reynolds, 1994) were studied on double polished section of fluorite from the mineralizing zone (Fig. 5c) in El-Missikat area. This study allowed determination of the physical state of the fluid (single- vs. two-phase), the type of fluid system (NaCl-H_2O, other major cations, presence and/or absence of condensed gases such as CO_2), fluid salinity and fluid density.

Fluid inclusion petrography

Most fluid inclusions (FI) are two-phase (liquid + vapor) at room temperature while few are single-phase (liquid). They are usually less than 60 μm in size and have variable shapes from oval, tabular and irregular. The vapor bubble occupies less than 20% of the total inclusion area. The inclusions are found in growth bands, along fracture planes, as three dimensional clusters and some appear isolated. Primary fluid inclusions in present fluorites are best identified by a relationship to growth zone boundaries (Fig. 5d).

Two types of FI have been recognized in El-Missikat fluorite crystals (Figs. 5d to g) according to their composition, shape, size and phase-type: Type A (high salinity aqueous FI) and Type B (low salinity aqueous FI). Generally Type A is two phases (H_2O vapor and liquid), rounded to lensoidal in shape, around 5-40 μm in size and characterized by high salinity and primary origin. Type B (low salinity) fluid inclusions are also aqueous, 5-60 um in size and irregular in shape, but they have low salinity and occur either on pseudosecondary trails or appear texturally primary. No microthermometric evidences of CO_2 have been found in any of the Fluid inclusion assemblages (FIA) of the present fluorites. For thermometric and LA-ICP-MS analyses (Fig. 5h), primary FI were selected.

Microthermometry

The data for all microthermometric measurements is given in Table 5 and Fig. 6. In type A FI, the final melting of ice (Tm ice) (Fig. 6a) is observed at temperatures between −13.5°C and −19.6°C (average, -16.2°C), corresponding to salinity (Fig. 6b) between 17.34 and 22.10 wt. % eq. NaCl (average, 19.4 wt.% eq. NaCl) (Bodnar and Vityk, 1994). Total homogenization (Th) (Fig. 6c) is achieved at temperatures between 201° C and 296°C (average, 232°C). All investigated inclusions homogenize into the liquid state. In type B FI (see Fig. 6), the Tm ice is observed at temperatures between −0.3°C and −2.7°C (average, -1.04°C), corresponding to salinity between 0.53 and 4.49 wt. % eq. NaCl (average, 1.80 wt. % eq. NaCl). Total homogenization is measured at temperatures between 160°C and 165°C 260 (average, 162°C).

Microthermometric measurements were carried out on the fluid inclusions to determine their salinity. This information was used as an internal standard to quantify the LAICPMS analyses (Heinrich et al., 2003). Homogenization experiments were preferably conducted after LA-ICPMS analyses on inclusions from the same assemblages that were not ablated to avoid potential destruction of the fluid inclusions before analyses.

The density of fluid inclusions can be obtained by plotting salinity versus homogenization temperature (Fig. 6d).Type B (low salinity FI) have a density of about 0.9 g/cm^3, lower than that in type B (high salinity FI) (0.9 to 1.0 g/cm^3).

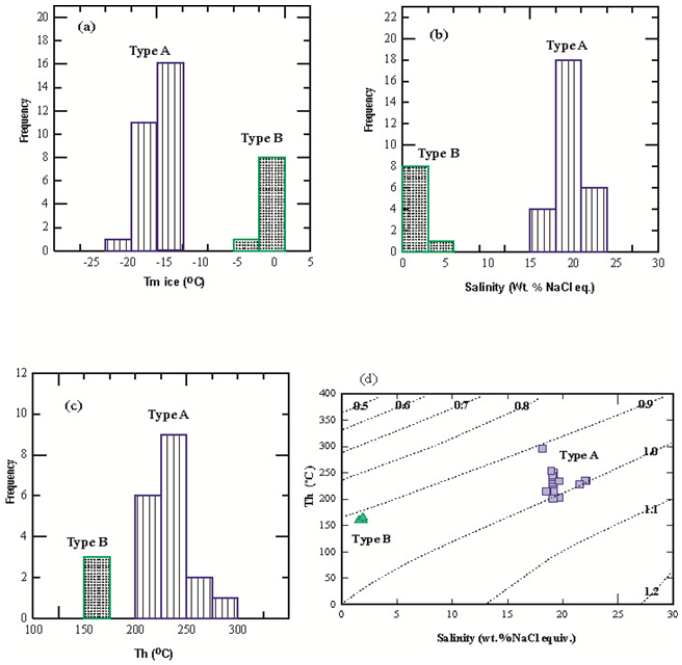

Fig. 6: Microthermometric results of fluorite mineralization in El-Missikat area. (a) Histogram of final melting point of ice (Tm^{o}C); (b) Histogram of the salinity equivalent (NaCl %); (c) Histogram of final homogenization temperatures (Th^{o}C); (d) Salinities (wt.% NaCl eqiv.) plotted against homogenization temperatures (Th^{o}C) after Wilkinson, 2001. Type A (high salinity fluids), Type B (low salinity fluids).

Laser-ablation-ICP-MS

Laser-Ablation Inductively-Coupled-Plasma Mass-Spectrometry (LA-ICP-MS) has become a very useful tool in the analysis of fluid inclusions, being a method to quantify the chemical composition of single fluid inclusions. The present work, for the first time, gives an idea about the element concentration in the fluid inclusion itself in fluorite in Egypt. Eleven fluid inclusions from Type A and Type B were analyzed for some special trace elements, Na, S, K, Ca, Fe, Cu, As, Sr, Y, Ag, Te, Cs, W, A, Pb, Th and U, via LA-ICP-MS. The results of these measurements are listed in Table 6.

To be able to compare the element concentrations of the different fluid inclusion types with each other a spider diagram was calculated using the average concentration of each element (Fig. 7). In general the high salinity FI (Type A) contains very high concentrations for almost all analyzed elements than that in the low salinity FI (Type B). The abundance of these elements is Ca > Na > S > K > Sr > Y > Fe, Pb > Cu > U > Cs, W, Te, Ag, As > Th > Au.

The concentration of Na in Type A (average 78622.8 ppm) is much higher than that in type B (average 7425.3 ppm). The K content of Type A ranges from 5595 to 19803 ppm, while of the Type B is low, 520 to 6766.9 ppm. The concentration of Sr in high salinity FI (Type A) lies between 2491.5 - 65844.3 ppm, which is higher than the concentration within the low salinity aqueous FI (149.4 - 1709.9 ppm).

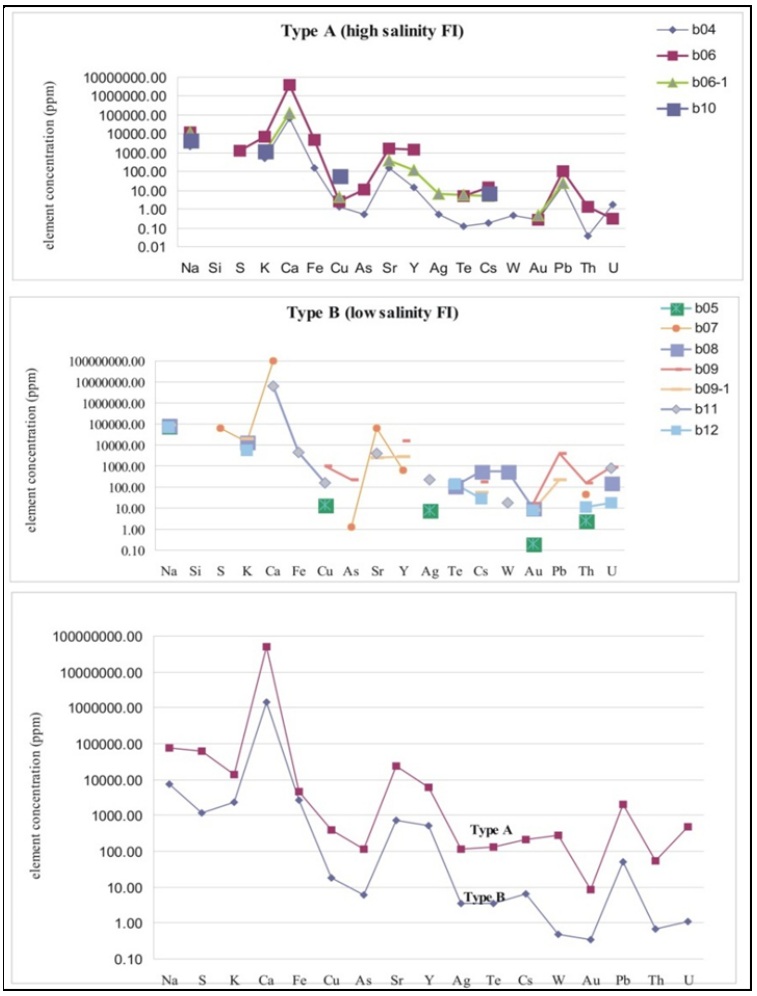

Fig. 7: Spider diagram showing the element concentrations per fluid inclusion type in El-Missikat fluorite.

The highest contents of Ag, Pb and Au (Table 6) are recorded in type A fluids (Ag=8.41to 217.7; Pb=222.8 – 3947.7 and Au=0.21 -16.3 ppm, respectively) while the lowest contents of these elements are present in Type B FI (Ag=0.5 – 6.7 ppm; Pb =18 – 102.9 and Zn=31-20 ppm). Also Y content is higher in Type A FI (600.8 -2711.5 ppm) than in the Type B FI (14 -1424.4 ppm.

The high salinity aqueous FI (Type A) contain more Fe, As, Te, Cs, W, Th and U (Table 6) than the low salinity aqueous FI (type B).

DISCUSSION

Genitic type and tectonic setting of the granitic host rock

The term “A-type” was first proposed by Loiselle and Wones (1979), to characterize granites of alkaline affinity, occurring in an anorogenic setting. Much evidence indicates that A-type granitoids, could occur both in postorogenic and anorogenic settings (Sylvester, 1989; Whalen et al., 1996; Pitcher, 1997). The El-Missikat granite exhibits geochemical characteristics typical of A-type granites (see Figs. 4c, e & f) such as low CaO, MgO, Sr, Ba and transition metals and high SiO_2, alkalis, Rb, Nb, Y and REE (Whalen et al., 1987; Bonin, 1990; El-Sayed, 1998).

The high Ga/Al ratios were proposed to be diagnostic mark of A-type granites (Whalen et al., 1987). Figure 8a shows the plots of the studied El-Missikat granite samples on the 10000*Ga/Al vs. Zr diagrams of Whalen et al. (1987). In this diagram, all the samples are discriminated as A type. In the (Y+Nb) vs. Rb and Rb vs. SiO_2 diagrams (Pearce et al., 1984), the studied samples plot in the within-plate granite field (Figs. 8b&c). Eby (1990, 1992) discriminated the A-type granites into A1 and A2 chemical subtypes, based on tectonic affinity (A1; truly anorogenic rifting, A2; post-collisional). Eby (1992) recommended the use of his A1 and A2 discrimination diagrams only for granitoids that plot in the field of within-plate granite of Pearce et al. (1984) and in the A-type granite field of the Ga/Al plots of Whalen et al. (1987). Therefore, the investigated granites are plotted on the (Nb – Y - Zr/4) and (Y/Nb vs. Rb/Nb) diagrams. Almost all the samples plotted in the post-collisional (A2) A-type granites (Figs. 8d&e). The El-Missikat granite show clear similarities to post-collisional granitoids (within-plate) from the Arabian–Nubian Shield. (Bentor, 1985; Katzir et al., 2007; Farahat et al., 2011; El-Bialy and Omar, 2015; Basta et al., 2017).

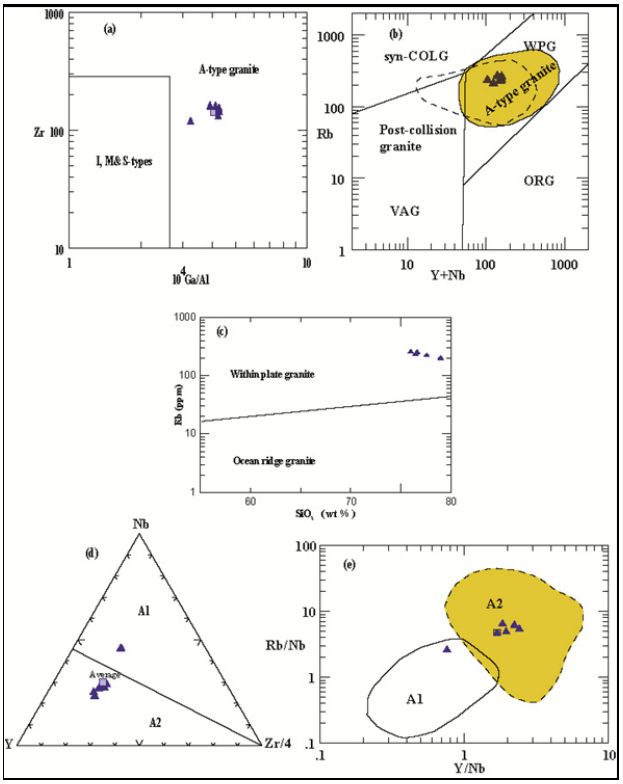

Fig. 8: Tectonic discrimination diagrams for the studied granite; (a) 10000* Ga/Al versus Zr diagram (Whalen et al. 1987); (b) Y + Nb vs. Rb tectonic discrimination diagram (Pearce et al. 1984). The A-type granites field is from Whalen et al. (1987); (c) SiO_2 vs. Rb diagram (Pearce et al. 1984); (d) Ternary Y-Nb-Zr diagram (Eby, 1992). A1= rift, plume and hotspot A-type granites and A2= post-collisional and post-orogenic A-type granites; (e) Y/Nb versus Rb/Nb discrimination diagram of Eby (1992) indicates A2-type affinity of these granites.

REY patterns

REE^{3+} can be incorporated into fluorites as Ca^{2+} replacement because of the similarity in ionic radius between REE^{3+} and Ca^{2+} (Elzinga et al., 2002). Fluorites may enrich REE from a fluid in which it is precipitated, thus the REE composition of fluorites can be used effectively in tracing the source of REE in ore-forming fluids. Moreover, fluorine is always enriched in the fluid where fluorite is precipitated and it is usual to observe REE-F complication in various hydrothermal environments (Wood, 1990; Hass et al., 1995).

Rare earth elements and Y (REY) are detectable in all fluorite samples from El-Missikat area (see Table 4); their contents show a wide range of variation from 33.9 to 329.3 ppm. The chondrite-normalized REY patterns are illustrated in Figure 9. Yttrium is inserted between Dy and Ho according to its ionic radius, its trivalent oxidation state, and its geochemical similarity to the REE. Generally, the chondrite-normalized patterns of all fluorites show enrichment in the HREEs compared with the LREEs, with strong Eu and Y anomalies. The highest total REE abundance have been observed in white and green varieties (average 203.2 and 200.9 ppm respectively), while the least abundance is recorded in the violet fluorite (average 75.5 ppm).

Genesis of fluorite mineralization

The ΣREE concentration in hydrothermal fluids is controlled by the pH and bulk chemical composition of solutions (e.g. Schwinn and Markl, 2005). Michard (1989) showed that the REE concentrations in fluids increase with decreasing pH. As outlined above, the average ΣREE content of Type V (violet) and Type G (green) & Type W (white) fluorite samples are 75.5, 200.9 and 203.2 ppm, respectively (i.e. increasing from violet fluorite to green and white fluorites; see Table 4). This feature implies that the differences in ΣREE in fluorite in the different fluorite types were possibly related to changes in pH condition. Generally, REE concentrations increase with decreasing pH (Michard, 1989). In alkaline fluids with carbonate species and/or halogens as complexing ligands, the HREE are enriched in solution and the REE patterns show a (La/Lu)n ratio <1 (Schwinn and Markl, 2005). From this point of view, it is assumed that the fluorite- bearing fluids were alkaline and HREE-enriched with respect to the LREE. Therefore, the fluorites deposited by those fluids should also be HREE-enriched. According to Möller (1991) an enrichment of the HREE in the REE patterns would indicate low Ca^{2+}/F ratios of the parent fluids. This means that the origin of the fluids must be from a F-rich source or from mobilization of previously existing fluorite mineralization in deeper parts of the crust (Lüders, 1991). This may apply to fluorites of El-Missikat area. There is close similarity in REY pattern of the present fluorites and Sardinian fluorites, Italy (group A) (Castorina et al. 2008) and other fluorite areas in the Eastern Desert of Egypt (Mahdy et al. 2013 and Fawzy, 2017).

Fleischer (1969) showed that the fluorites from a single location may exhibit different REE abundances, controlled by the variability of the parameters governing the mineralizing process. However, comparing the REY patterns of the El-Missikat fluorites with those of the most common types of fluorite of various origins (e.g. Möller et al., 1998), it is evident that the present fluorites were deposited by hydrothermal fluids.

Among physical–chemical conditions controlling REE concentrations, it is considered that Tb and Gd are the REE which establish the most stable complexes with F. This leads to some enrichment of Gd and Tb in hydrothermal fluids (Wood, 1990). The patterns of the present fluorites may be explained by a weaker F complication of Gd and Tb, probably because the fluorite deposition took place at early stage of the hydrothermal process. In contrast, crystallization during a late stage of the hydrothermal process gave a normalized convex REY pattern (Castorina et al., 2008).

All types of fluorite in El-Missikat area exhibit Eu, Y, and Ce anomalies (Figs. 9a to c). These anomalies are indicative of the mode of deposition of the mineral (Möller et al., 1998). The negative Eu anomalies in the present fluorite have crystallized at temperatures above 200°C (Bau 1991; Möller et al., 1998; Möller and Holzbercher1998; Schwinn and Markl 2005). The Eu anomaly is controlled thermally and chemically, mainly by redox conditions. Generally, the Eu^{3+}/Eu^{2+} redox potential of hydrothermal fluids depends strongly on temperature; at T>200 °C, Eu^{3+} is reduced to Eu^{2+}, the size of Eu^{2+} prevents its incorporation into the fluorite lattice, and, thus, the fluorite will show a negative Eu anomaly due to a crystallographically controlled fractionation during precipitation. The negative Eu anomaly in the fluorite indicates its depletion in the medium under which fluorite was formed. The late magmatic melt is diagnostically deficit in Eu (Gill, 1996). The negative Eu anomalies in the fluorites mostly indicate a late magmatic origin which shows HREEs enrichment than LREEs (Bulnayev and Kaperskaya, 1990). Yttrium anomalies reflect fluid complexation with F (Möller et al., 1998). The positive Y anomalies indicate strong complexation with F, and decoupling of Y from HREE is a common feature in hydrothermal fluids dominated by F complexes (Möller et al., 1998; Schönenbeger et al., 2008)**.** The slightly negative Ce or chondritic Ce anomalies of the El-Missikat fluorites and associated host rock (Fig. 9d) suggest that the parent fluids interacted with rocks under reducing conditions or with weakly oxidizing fluids (Möller et al., 1998).

Tb/Ca and Tb/La ratios

According to Constantopoulos (1988) and as a result of the different stabilities of the REE complexes, early formed fluorite is La-rich and Tb-poor (lower Tb/La ratio). As crystallization proceeds, the fluorine concentration of the fluid is rapidly depleted, which leads to the decomposition of TbF^{2+} and the other rare

earth-fluoro complexes. Since much of the La has already been taken up, late-stage fluorite will be relatively Tb-rich and the fluorite will have a higher Tb/La ratio. The values of Tb/La ratios (see Table 4) indicate that the violet variety has the lowest Tb/La ratio (0.132 to 0.890, average = 0.430 ppm), which is indicative of earlier crystallization. The high Tb/La ratio in the green (0.16 to 3.72, average =1.47 ppm) and white fluorite (0.12 to 3.65, average = 1.25 ppm) varieties indicate that they crystallized from more evolved fluids (late stages of the evolution of the hydrothermal fluids) (Constantopoulos, 1988). The Tb/Ca ratio has also been used as an environmental index, since REE contents were found to vary with Ca concentrations (Möller et al., 1976; Möller and Morteani, 1983). In addition, it has been demonstrated that the magnitude of the Tb/Ca ratio relative to the Tb/La ratio in a fluorite could be used as a criterion for the genesis of this mineral (Jacob, 1974).

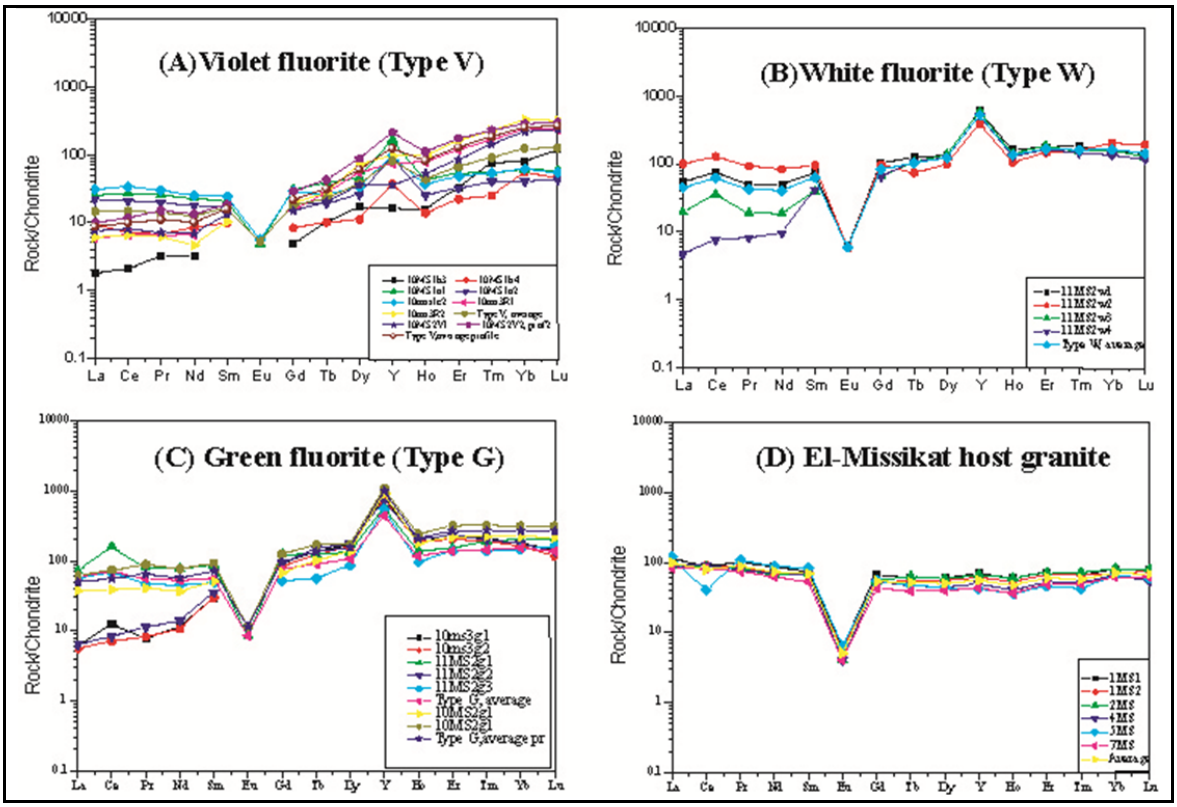

Fig. 9: Chondrite- normalized REY patterns for the samples of fluorite and associated host granitic rock in El-Missikat area.

Möller et al. (1976) used the Tb/Ca–Tb/La diagram to distinguish fluorites of pegmatitic from hydrothermal or sedimentary origin. On this diagram, fluorite was assumed to be stoichiometrically composed of calcium and fluorine. The small amount of trace elements incorporated into fluorite does not change the overall position of data points in the diagram as discussed by Gagnon et al. (2003). All fluorite types from El-Missikat area plot within the hydrothermal field (Fig. 10). Most of the samples appear to illustrate a fractionation trend in which Tb/La ratios increase with the Tb/Ca, producing a trend parallel to the field boundaries (Möller et al., 1976). Moreover, from the relative position of the El-Missikat fluorite in the Möller et al. (1976) variogram, it can be derived that the less fractionated fluorite (violet pocket-shaped bodies, Type V) was deposited relatively earlier than the green- whitish fluorite during the mineralizing process (Type G & Type W).

Y–Ho fractionation

The mean Y content of the fluorite samples in El-Missikat area increases from 128.5 ppm in Violet fluorite , through 819.6 ppm in white fluorite, to 823.7 ppm in green florite, with the Y/Y* ratios ranging from 0.97-3.73 (average= 2.02) through 3.90-4.16 (average= 4.05) to 1.89-5.95 (average= 3.96), respectively (see Table 4). The pronounced positive Y anomalies in these fluorite samples are suggestive

of strong Y−Ho fractionation in the El-Missikat hydrothermal system. Möller (1998) linked significant enrichment in Y to the presence of fluoride complexing agents, and Bau (1996) proposed that Y–F complexes are more stable than Ho–F complexes. Therefore, Y preferentially remains in F-rich fluids, and fluorite deposited from fluids has increasing Y contents and Y/Y* ratios from the early to late mineralization stages. In Type G (green fluorite) which have a wide range of Y\Y* due to the pocket-shape bodies was deposited relatively earlier than the vein fluorite.

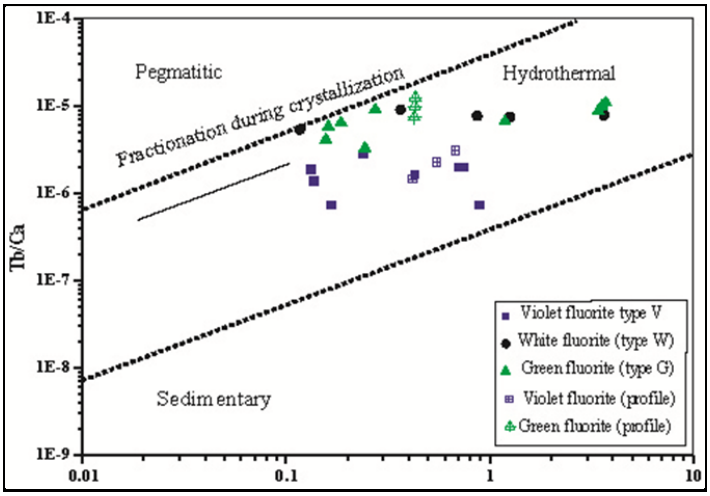

Fig. 10. The Tb/Ca versus Tb/La relationship in the present fluorite (field is after Moller et al., 1976).

Bau and Dulski (1995) studied the fluorite and calcite from the Tannenboden and Beihilfe deposits and concluded that variations in Y/Ho ratio in cogenetic hydrothermal fluorites are usually almost negligible compared with those of La/Ho ratios. The Y/Ho ratios of fluorite samples from the El-Missikat deposit (Fig. 11) range from 26.58 - 107.3 (average=61.97) through 102 - 112.7 (average=107.4) to 50.8 – 157 (average=103.81) in the violet, white and green varieties respectively (see Table 4). The Y/Ho ratios of all samples obviously higher than those of chondrites (Y/Ho ratios=28, Anders and Grevesse, 1989), confirming that these fluorites are of hydrothermal origin similar to other hydrothermal fluorite. El-Kammar et al. (2001), mentioned that the mass balance of Gattar granite suggested losses for Y due to alteration and their liberation from metamictized accessory minerals into the fluids.

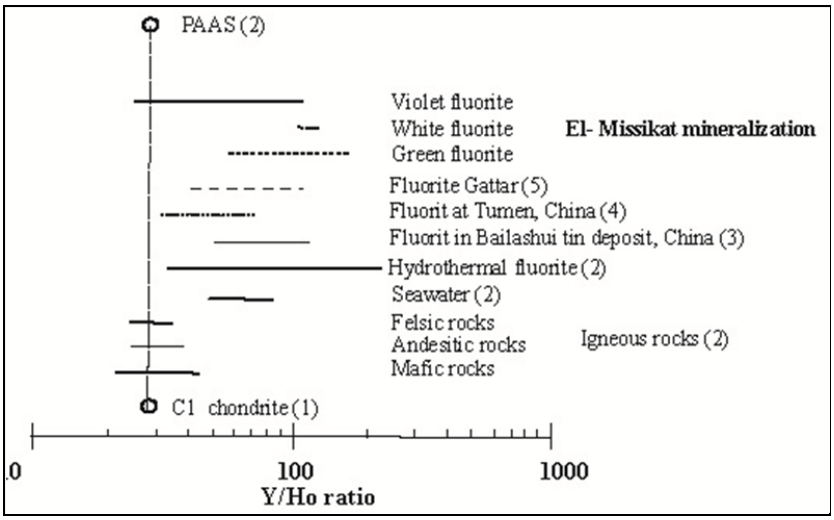

Fig. 11. Comparison of the Y/Ho ratios of the present fluorite with other kinds of geological bodies. Data after, (1) Anders and Grevesse (1989), (2) Bau and Dulski (1995), (3) Shunda et al. (2008), (4) Deng et al. (2014) and (5) Mahdy et al. 2013.

The fluorites in the present area have positive Y anomalies and increasing Y/Ho ratio (Fig. 12). These characteristics indicate that the present fluorite deposited from interaction of a fluorine-rich aqueous fluids with the host rock (Bau and Dulski 1995).

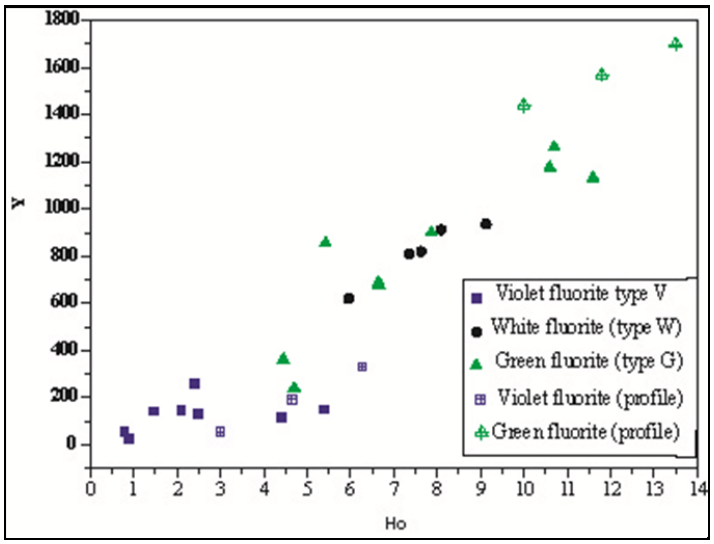

Fig. 12. Binary variation diagram of Y vs Ho of the studied fluorites

Source of REE and fluid chemistry

The El-Missikat fluorites and host granite are generally characterized by a strongly negative Eu, positive Y, and slightly negative or chondritic Ce anomalies. The REY patterns of the fluorite and host granite are almost similar (see Fig. 9). This indicates that the source of REE and F in the hydrothermal solutions could be the host granite leached by fluids (Shunda et al., 2008; Mahdy et. al., 2013 and Deng et al., 2014). The slight Ce anomalies of the fluorites and the host El-Missikat granite suggest that the parent fluids reacted with the granite in reduced or weakly oxidized conditions. Eu/Eu*, Ce/Ce*, and Y/Y* patterns prove that fluorite records the compositional evolution of the hydrothermal solutions that had transported the trace and REE from the host granite during the fluid–wall rocks interactions.

The fluid inclusions of the fluorite have homogenization temperatures ranging from 201^{o}C to 296^{o}C in Type A (high salinity FI) and 160^{o}C to 165^{o}C in Type B **(**low salinity FI). The melting temperature of ice in fluorite indicates salinities of up to 19.4 equiv. wt% Na CI (Type A) but Type B FI have a low range of salinity (0.53 to 4.49 equiv. wt% Na Cl). The density of fluid inclusions is obtained by plotting salinity versus homogenization temperature (see Fig. 6d). Fluid inclusions of type A (high salinity FI) have a density ranging from 0.9 to 1.0 g/cm^3. The low salinity FI (Type B) has a density of 0.9 g/cm^3.

From the LA-ICP-MS data for the individual fluid inclusions of El-Missikat fluorite (see Table 6) , it is clear that the high salinity FI (Type A) contains very high concentrations for almost all analyzed elements than that in low salinity FI (Type B). It seems that the high salinity fluids (related to granitic magma) is the main source for almost all elements in the present mineralization. The abundance of the analyzed elements in fluid inclusions from El-Missikat fluorite is Ca > Na > S > K > Sr > Y > Fe, Pb > Cu > U > Cs, W, Te, Ag, As > Th > Au.

The elements content in the studied fluid inclusions are compared to worldwide published values for selected fluorites (Table 7). The analyzed concentrations of Fe, pb, Ag, Na and K in present FI are similar to those reported in comparable hydrothermal veins and Missisippi Valley type deposits (MVT), but higher than in most present-day sedimentary brines.

Fluid inclusion data has been widely used to confirm the geochemical data about the origin and source of fluid for ore deposits. As it is clearly shown from the fluid inclusion studies that it is possible to define two different ore-forming solutions. The first one is marked by high salinity (type A) and is comparable with the fluids described for other hydrothermal systems of the European Hercynian basement (basement brines) (Behr et al., 1987; Zak et al., 1990; Luiders et al., 1993). The second fluid is characterized by low salinity (type B) and could be considered as convecting formation waters (evolved surficial waters).

During extensional events, the downward penetration of surface fluids into basement rocks may occur along fault zones (Oliver et al., 2006). These fluids can leach metals from the basement and transport

them; leading to the formation of hydrothermal ore deposits in the basement and/or the overlying cover sequences. In fact, many hydrothermal ore deposits from sedimentary basins have isotopic and geochemical signatures that point to an involvement of basement rocks, particularly as a source of metals (e.g. Shelton et al., 1995).

The deposition mechanisms for fluorite may be 1) fluid mixing, 2) changes in pressure and temperature and 3) fluid-rock interaction (Richardson and Holland, 1979). Thus, the possibility of fluid mixing as fluorite depositional mechanism still remains. This fluid gives evidences for forming F mineralization in El-Missikat area. In the case of present saline fluid in El-Missikat fluorite, the drop in temperature combined with the fluid inclusion composition lead to changes in fluorite solubility (Richardson and Holland, 1979). Thus cooling cannot be excluded as possible deposition mechanism. The strong positive Y anomaly and negative Eu anomaly indicate a high temperature of the fluid and change in their phsico-chemical potential. The remobilization and precipitation of many rare metals (Nb, Zr, REE+Y and chalcophile elements), are due to the change in Ph condation (El Kammar et al., 2001). The intense wall rock alterations associated with fluorite mineralization such as hematitization and kaolinization are good evidences for interaction between the hydrothermal fluids and the country rocks.

Origin of fluorite coloration

Natural fluorites exhibit the largest variety of colours. Several theories have been proposed to explain the cause of these colorations since the first studies on this subject (Mollow, 1934 and Przibram, 1956), who made detailed studies of natural and irradiated fluorites and compared the results with those on similarly treated synthetic crystals, followed by extensive work on synthetic CaF_2 crystals. Serra (1947) and Allen (1952) attributed the colors in fluorite to the role of the REE during the differentiation of magma or due to the presence of manganese. Sierro (1963) reported the R-centre (colour centre element) in coloured fluorites. The R-centre in fluorite is an association of an yttrium ion with two oxygen ions placed as an impurity in the crystal and ionised in course of time by natural radiation. Bill et al. (1967) attributed the red colour of fluorite to the presence of (YO_2) complex and the green colour to the presence of Sm^{+3} and the colour disappeared by heating to 300^{o}C. Mackenzie and Green (1971) have studied the physical properties and chemical constitution of various Blue John fluorites and ascribed their colour to the presence of colloidal and sub-colloidal conglomeration of calcium atoms in the fluorite lattice. Bill and Calas (1978) studied the natural coloured fluorites by means of optical absorption and electron paramagnetic resonance and found complex centers involving rare-earth ions and / or oxygen giving rise to the various colours including yttrium-associated *F* centers (blue), coexisting yttrium and cerium-associated *F*- centers (yellowish-green), (YO_2) center (rose) and the O^{3-} molecule ion (yellow). Galway et al. (1979) suggested that, the blue zones consist of colloidal calcium resulting from radiation damage caused by the intermittent deposition of radioactive material on the surface of fluorite during crystal development. Rasmy et al., (1992) concluded that the blue-violet fluorite in El-Missikat uranium vein is due to the presence of colour centre element (rare earth element). El-Kammar et al. (1997) studied fluorites from El-Erediya and El-Missikat and came to the conclusion that the change in colour is controlled by the Y content in particular, and the Y-group in general. The Y content increases from 0.06 mol. per unit cell of colorless fluorite to 0.15 mol. per unit cell for violet fluorite. El-Mansi (2000) concluded that Sr is responsible for the appearance of colourless to rather white colour while Y is responsible for the green colour. Also he mentioned that, the blue and mauve varieties are generally high in U and Th contents.

A review of the literature shows that there are four groups of models which try to explain the violet colour: (1) inclusions of organic compounds, (2) some kind of impurity defects as Mn^{2+}, REE^{3+}, or REE^{2+}, (3) colloids of metallic Ca formed under radioactive irradiation, (4) some kind of hole or electron centre with the charge trapped somewhere in the lattice.

The present work revealed that green and whitish fluorite have higher contents of Y (average=823.7 ppm and 819.6 ppm, respectively) than that in violet fluorite (Y=128.5 ppm) indicating that the Y content act as colour centre element for greenish fluorite. Also the REE content is higher in green (average=200.95) ppm and white (average =203.02 ppm) fluorites than that in the violet type (average

75.47 ppm). In contrast, distribution of Sr indicates that, the violet fluorite varieties have higher Sr contents (average=431.9 ppm) than the white (average=84.3ppm) and green (average= 70.01 ppm) fluorites. It can conclude that the abundance of Y and REE are a characteristic for the greenish-white fluorite, but they are much less in violet fluorite which has high Sr contents.

CONCLUSIONS

From the foregoing the following concluding remarks can be drawn:

1-Green (Type G), white (Type W) and violet (Type V) fluorites occurs as disseminations and veinlets in the host granitic rocks in El-Missikat area, central Eastern Desert, Egypt. Petrographically, the host granite represented by biotite granite. Mineral chemistry data of primary phases are given. Plagioclase is albite (average 2.79 mol%). The composition range of orthoclase is $An_{0.02\ to\ 0.42}$, $Ab_{1.56\ to\ 10.1}$ $Or_{83.4\ to\ 98.3}$ mol%. Biotite is primary magmatic origin and crystallized at 500 - 600°C. Geochemically, El-Missikat granite is peraluminous A- type and was generated in post-collision environment (within-plate).

2-Fluorites from the El-Missikat area are the products of interactions between hydrothermal fluids associated with granitic magmatism and the host rock; the REE and F in the ore-forming fluid are derived mainly from the younger host rock.

3-Generally, the chondrite-normalized patterns of all fluorites show enrichment in the HREEs compared with the LREEs. The highest total REE abundance have been observed in white and green varieties (average 203.2 and 200.9 ppm respectively), while the least abundance is recorded for the violet fluorite (average 75.5 ppm). The ΣREE concentration in hydrothermal fluids is controlled by the pH and bulk chemical composition of solutions.

4- All types of fluorite in El-Missikat area exhibit strong Eu, Y, and slight Ce anomalies. The negative Eu anomalies in the present fluorite suggested that they crystallized at temperatures above 200°C (late magmatic origin, Bulnayev and Kaperskaya, 1990). Positive Y anomalies indicate strong complexation with F, and decoupling of Y from HREE is a common feature in hydrothermal fluids dominated by F complexes (Möller et al., 1998; Schönenbeger et al., 2008)**.** The slightly negative Ce or chondritic Ce anomalies of the El-Missikat fluorites and associated host rock suggested that the parent fluids interacted with rocks under reducing conditions or with weakly oxidizing fluids (Möller et al., 1998).

5-The Tb/Ca and Tb/La ratios in the studied fluorite confirmed that the REE were progressively incorporated into the fluorites during hydrothermal mineralization. The Y/Ho ratios are typical of hydrothermal fluorites that were likely formed by the interaction of magmatic fluids with the granitic wall-rocks.

6- Two types of FI have been recognized in El-Missikat fluorite crystals: Type A (high salinity aqueous FI) and Type B (low salinity aqueous FI). The homogenisation temperatures ranging from 20°C to 296°C in Type A and 160°C to 165°C in Type B. The melting temperature of ice in fluorite indicates salinities of up to 19.4 equiv. wt% Na CI in Type A but Type B FI have a low range of salinity (0.53 to 4.49 equiv. wt% Na Cl). Fluid inclusions of type A have a density ranging from 0.9 to 1.0 g/cm^3 but the density of Type B is 0.9 g/cm^3.

7- The present work, for the first time, gives an idea about the element concentration in the individual fluid inclusion in fluorite in Egypt. In general the high salinity FI (Type A) contains very high concentrations for almost all analyzed elements than that in the low salinity FI (Type B). The abundance of these elements is Ca > Na > S > K > Sr > Y > Fe, Pb > Cu > U > Cs, W, Te, Ag, As > Th > Au. The analyzed concentrations of most elements (e.g. Fe, Pb, Ag, Na and K) in studied FI are similar to those reported in comparable hydrothermal veins and Missisippi Valley type deposits, but higher than in sedimentary brines.

8- Mixing of low salinity meteoric water (Type B) with hot high saline hydrothermal solution (Type A) leads to pH change and continuous interaction with wall-rock. Therefore the mechanism of fluorite precipitation is accompanied with alteration processes.

9-The green and whitish fluorite have higher contents of Y (average=823.7 ppm and 819.6 ppm, respectively) than that in violet fluorite (Y=128.5 ppm) indicating that the Y content act as colour centre element for greenish-white fluorite. The contents of Y may be responsible for the appearance of green and white. Sr may be responsible of fluorite violet colouration (Type V, average=431.9 ppm; Type W, average=84.3ppm; Type G, average= 70.01 ppm).

ACKNOWLEDGEMENTS

I express my gratitude to Prof. Dr. C. Heinrich, ETH-Zurich, Switzerland, for the laboratory facilities. I thank Prof. Dr. Peter Ulmer, Prof. Dr. Eric Reusser, Dr. Markus Wälle and Lydia Zehnder, ETH-Zurich, for the help in geochemical and microprobe analyses. I am greatly indebted to Ass. Prof. A. E. Maurice, Geology Dept., Helwan University, for help in the field.

REFERENCES

Abdel-Rahman, A.M., (1994): Nature of biotites from alkaline, calc-alkaline and peraluminous magmas. Journal of Petrology 35, 525–541.

Ali, B. H. (2001): Trace elements distribution and fluid inclusions studies of fluorite: Evidence for hydrothermal alteration in Gabal Gattar area, North Eastern Desert, Egypt. Egypt. J. Geol., 45/2, 1003-1015.

Allen, R. D. (1952): Variation in chemical and physical properties of fluorite. Amer. Min., 37, 910-930.

Anders E. and Grevesse N., (1989): Abundances of the elements: Meteoritic and solar. Geochim. Cosmochim. Acta, 53, 187–214.

Abu Dief, A., Ammar, S. E. and Mohamad, N. A. (1997): Geological and geochemical studies of black silica at El-Missikat pluton, Central Eastern Desert, Egypt. Proc. Egypt. Acad. Sci. 47: 335-346.

Bakhit, F. S. (1978): Geology and radioactive mine-ralization of Gabal EL-Missikat area, Eastern Desert, Egypt. Ph.D. Thesis, Faculty of Science, Ain Shams Univ., Cairo, 1-289.

Bakhit, F. S. and EL Kassas, I. A. (1989): Distribution and orientation of radioactive veins in the El Erediya-El Missikat area, Central Eastern Desert, Egypt, International Journal of Remote Sensing, 10/3: 565-581.

Barbieri, M., Masi, VOL., and Tolomeo, L. (1984): Strontium geochemical evidence for the origin of the deposits from Sardinia, Italy. Econ. Geol., 79, 1360-1365.

Basta, F.F., Maurice, A.E., Bakhit, B.R., Ali, K.A. and Manton, W.I. (2011): Neoproterozoic contaminated MORB of Wadi Ghadir Ophiolite, NE Africa: Geochemical and Nd and Sr isotopic Constraints. J. Afr. Earth Sc. 59, 227–242.

Basta, F.F., Maurice, A.E., Bakhit, B.R., Azer, M.K. and El-Sobky, A.F. (2017): Intrusive rocks of the Wadi Hamad area, North Eastern Desert, Egypt: change of magma composition with maturity of Neoproterozoic continental island arc and the role of collisional plutonism in the differentiation of arc crust. Lithos 288–289, 248–263.

Bau, M. (1991): Rare earth element mobility during hydrothermal and metamorphic fluid–rock interaction and the significance of the oxidation state of Europium. Chem Geol 93, 219–230.

Bau, M. (1996): Controls on the fractionation of isovalent trace elements in magmatic and aqueous systems: evidence from Y/Ho, Zr/Hf, and lanthanide tetrad effect. Cont. Min. Pet., 123, 323–333.

Bau M. and Dulski P. (1995): Comparative study of yttrium and rare earth element behaviors in fluorine-rich hydrothermal fluids. Cont. Min. Pet., 119, 213–223.

Behr, H.J., Horn, E.E., Frentzel-Beyme, K. and Reutel, Chr. (1987): Fluid inclusion characteristics of the Variscan and post-Variscan mineralizing fluids in the Federal Republic of Germany. In: EB. Horn and H.-J. Behr (Guest-Editors), Current Research on Fluid Inclusions, ECRFI, Gettingen, April.

Bentor, Y. K. (1985): The crustal evolution of the Arabo-Nubian Massif with special reference to the Sinai Peninsula. Precamb. Res., 28, 1–74.

Bill, H. and Calas, G. (1978): Color centres associated rare earth ions and the origin of coloration in natural fluorites. Phys Chem. Min., 3, 117-131.

Bill, H., Sierro, J. and Lacroix, R. (1967): Origin of colouration in some fluorites. Amer. Miner., 52, 1003-1008.

Bodnar, R. J. and Vityk, M. O. (1994): Interpretation of microthermometric data for H_2O–NaCl fluid inclusions. In: De Vivo, B., Frezzotti, M.L. Eds.., Fluid Inclusions in Minerals: Methods and Applications. Short Course of the Working Group IMA. 'Inclusions in Minerals', September 1–4, 1994, Pontignano- Siena, 117–130.

Bonin, B. (1990): From orogenic to anorogenic settings: evolution of granitoid suites after major orogenesis. Geol. J. 25, 261–270.

Bouch, J. E., Naden, J., Shepherd, T. J., McKervey, J. A., Young, B., Benham, A. J. and Sloane, H. J. (2006): Direct evidence of fluid mixing in the formation of stratabound Pb–Zn–Ba–F mineralisation in the Alston Block, North Pennine Orefield (England). Mineralium Deposita 41 (8), 821–835.

Bulnayev, K. B. and Kaperskaya, Yu. N. (1990): Trends in the REE distribution in fluorite from various types of deposits in Transbaykalia. Transl. Geokhimya 12, 1742-1755.

Caballero, J.M., Casquet, C., Galindo, C., Gonzalez-Casado, J.M., Snelling, N. and Tornos, F. (1992): Dating of hydrothermal events in the Sierra del Guadarrama, Iberian Hercynian Belt (Spain). Geogaceta 11, 18–22.

Carpenter, A.B., Trout, M.L. and Picket, E.E. (1974): Preliminary report on the origin and chemical evolution of lead- and zinc–rich oil field brines in Central Mississippi. Econ. Geol., 69 (8), 1191–1206.

Castorina F., Masi U., Padalino G. and Palomba, M. (2008): Trace-element and Sr–Nd isotopic evidence for the origin of the Sardinian fluorite mineralization (Italy), Applied Geochemistry 23, 2906 –2921.

Collins, W. J., Beams, S. D. and White, A. J. R. et al. (1982): Nature and origin of A- type granites with particular reference to southeastern Australia, Cont. Min. Pet., 80: 189-200.

Constantopoulos, J. (1988): Fluid inclusions and rare earth elements geochemistry of fluorite from South-Central Idaho. Econ. Geol., 83, 626-636.

Deng, X.H., Chen,Y. J., Yao, J. M., Bagas, L. and Tang, H. (2014): Fluorite REE-Y (REY) geochemistry of the ca. 850 Ma Tumen molybdenite–fluorite deposit, eastern Qinling, China: Constraints on ore genesis, Ore Geology Reviews 63, 532-534.

Eby, G. N. (1990): The A-type granitoids: a review of their occurrence and chemical characteristics and speculations on their petrogenesis. Lithos 26, 115–134.

Eby, G. N. (1992): Chemical subdivision of the A-type granitoids: petrogenetic and tectonic implications. Geology 20, 641–644.

Eggins, S.M. (2003): Laser ablation ICP-MS analysis of geological materials prepared as lithium borate glasses. Geostandards Newsletter 27 (2), 147–162.

Eliwa, H.A., Breitkreuz, C., Murata, M., Khalaf, I.M., Bühler, B., Itaya, T., Takahashi, T., Hirahara, Y., Miyazaki, T., Kimura, J.I., Shibata, T., Koshi, Y., Kato, Y., Ozawa, H.,

El-Bialy, M.Z. and Omar, M.M. (2015): Spatial association of Neoproterozoic continental arc I type and post-collision A-type granitoids in the Arabian–Nubian Shield: the Wadi Al- Baroud Older and younger granites, North Eastern Desert, Egypt. J. Afr. Earth. Sci. 103, 1–29.

El Hadek, H., Mohamed, A.M., Bishara, W.W., El Habaak, G.H. and Ali, K.A. (2016): Evolution of mineralizing fluids of greisen and fluorite veins, evidence from fluid inclusions. Int. J. Geophys. Geochem. 3 (5), 49-56.

El-Kammar, A.M., El-Hazik, N., Mahdi, M. and Aly, N. (1997): Geochemistry of accessory minerals associated with radioactive mineralization in the Central Eastern Desert, Egypt. J. Afr. Earth Sci. 25 (2), 237-252.

El-Kammar A. M., Salman A. E., Shalaby M. H. and Mahdy A. I. (2001): Geochemical and genetical constraints on rare metals mineralization at the central Eastern Desert of Egypt. Geochem. J, 35, 117-135.

El-Mansi, M. M. (1993): Petrology, radioactivity and mineralizations of Abu Gerida - El- Erediya area, Eastern Desert, Egypt. M.Sc. Thesis, Cairo Univ., 223p.

El-Mansi, M. M. (2000): Coloration of fluorite and its relation to radioactivity. Egypt. Mineral., 12, 93-106.

El-Sayed, M. M. (1998): Tectonic setting and petrogenesis of the Kadabora pluton: a late Proterozoic anorogenic A-type younger granitoid in the Egyptian Shield. Chem Erde 58: 38–63.

Elzinga E. J., Reeder R. J., Withers S. H., Peale R. E., Mason R. A., Beck, K. M. and Hess W. P. (2002): EXAFS study of rare-earth element coordination in calcite. Geochim. Cosmochim. Acta, 66, 2875-2885.

Farahat, E. S., Zaki, R., Hauzenberger, C. and Sami, M. (2011): Neoproterozoic calc-alkaline peraluminous granitoids of the Deleihimmi pluton, Central Eastern Desert, Egypt: implications for transition from late- to post-collisional tectonomagmatic evolution in the northern Arabian-Nubian Shield. Geol. J. 46 (6), 544-560.

Fawzy, Kh. M. (2001): Mineral composition and geochemistry of barite-fluorite mineralization at Wadi el-sodmein, central eastern Desert, Egypt. Egypt. Mineral. 13, 27-43.

Fawzy, Kh. M. (2017): Characterization of a post orogenic a-type granite, gabal El Atawi, central eastern Desert, Egypt: geochemical and radioactive perspectives. Open J. Geol. 7, 93-117.

Fawzy, Kh. M., Solovova, I. P., Babanskii, A. D. and Ryabchikov, I. D. (1996): Formation conditions of veined fluorite (Homrat Akarem, Egypt) inferred from an inclusion study. Geochem. Int. 14 (1), 32-35.

Fleischer, M. (1969): The lanthanide elements in fluorite. Indian Mineral, 10, 36–39.

Frape, S.K. and Fritz, P. (1987): Geochemical trends from groundwaters from the Canadian Shield. In: Fritz, P., Frape, S.K. (Eds.), Saline water and gases in crystalline rocks. Geological Association of Canada Special Paper, 33, 19-38.

Frost, B.R., Barnes, C.G., Collins, W.J., Arculus, R.J., Ellis, D.J. and Frost, C.D. (2001): A geochemical classification for granitic rocks. J. Petrol. 42 (11), 2033-2048.

Gagnon, J. E., Samson, I. M., Fryer, B. J., Williams-Jones, A. E., (2003): Compositional heterogeneity in fluorite and the genesis of fluorite deposits: insights fromLA-ICP-MS analysis. Can. Mineral. 41, 365–382.

Galway, A. K., Johnes, K. A. and Reed, R. (1979): The blue colouration in banded fluorite (blue John) from Castleton, Derbyshire, England. Min. Mag. 43, 243-250.

Gill, R., 1996. Chemical Fundamentals of Geology. Harper Collins academic publishers, London & New York, p. 291.

Gokhale, N. W. (1968): Chemical composition of biotite as a guide to ascertain the origin of granites. Bull. Soc. Geol. Final., 40, 107-111.

Goldstein, R.H., and Reynolds, T.J. (1994): Systematics of fluid inclusions in diagenetic minerals: Tulsa, Oklahoma, Society for Sedimentary Geology, 199 p.

Guillong, M., Latkoczy, C., Seo, J. H., Günther, D. and Heinrich, C. A. (2008): Determination of sulfur in fluid inclusions by laser ablation ICP-MS, J. Anal. At. Spectrom. 23, 1581-1589.

Günther, D., Audétat, A., Frischknecht, R. and Heinrich, C.A. (1998): Quantitative analysis of major, minor and trace elements in fluid inclusions using Laser Ablation-Inductively Coupled Plasma-Mass Spectrometry (LA-ICP-MS). J. Anal. At. Spectrom.13, 263-270.

Halter, W. E., Pettke, T., and Heinrich, C. A. (2002): The origin of Cu/Au ratios in porphyry-type ore deposits: Science, 196, 1844-1846.

Hass J. R., Shock E., and Sassani D. C. (1995): Rare-earth elements in hydrothermal systems: Estimates of standard partial molal thermodynamic properties of aqueous complex of the rare earth elements at high pressures and temperatures. Geochim. Cosmochim. Acta, 59, 4329-4350.

Heinrich, C.A., Pettke, T., Halter, W.E., Aigner-Torres, M., Audétat, A., Günther, D., Hattendorf, B., Bleiner, D., Guillong, M. and Horn, I. (2003): Quantitative multi-element analysis of minerals, fluid and melt inclusions by laser-ablation inductively-coupled plasma mass-spectrometry. Geochim. Cosmochim. Acta 67, 3473-3497.

Henry, D. J., Guidotti, C.V. and Thomson, J. A. (2005): The Ti-saturation surface for low-to-medium pressure metapelitic biotites: implications for geothermometry and Ti substitution mechanisms Am. Mineral. 90, 316-328.

Hussein, A. A. (1990): Mineral deposits of Egypt, in Said R. (1990), Geology of Egypt, Ch. 26, 511-566.

Hussein, H. A., Hassan, M. A, EL-Tahir, M. A. and Abu Deif, A. (1986): Uranium bearing siliceous veins in younger granites, Eastern Desert, Egypt. International Atomic Energy Agency (IAEA), Tecdoc 361, 143-157.

Jacob, K. H. (1974): Deutung der genese von fluoritlagerstatten anhand ihrer spuren elemente-insbesondere an fraktionierten seltenen Erden. Ph.D. dissertation, Technology Univesity, Berlin, Germany.

Jochum, K. P.,Willbold, M., Raczek, I., Stoll, B. and Herwig, K. (2005): Chemical characterization of the USGS reference glasses GSA-1G, GSC-1G, GSD-1G, GSE-1G, BCR-2G, BHVO-2G and BIR-1G using EMPA, ID-TIMS, ID-ICP-MS and LA-ICP-MS. Geostandards and Geoanalytical Research 29 (3), 285-302.

Katzir Y., Eyal M., Litvinovsky B. A., Jahn B. M., Zanvilevich A.N., Valley J.W., Beeri Y., Pelly I. and Shimshilashvili E. (2007): Petrogenesis of A-type granites and origin of vertical zoning in the Katharina pluton, Gebel Mussa (Mt. Moses) area, Sinai, Egypt, Lithos 95, 208-228.

Loiselle, M. C. and Wones, D. R. (1979): Characteristic and Origin of anorogenic granites, Geol. Soc. Am. Abstr. Prog., 11, 468.

Lüders, V. (1991): Formation of hydrothermal fluorite deposits of the Harz Mountains, Germany. In: Pagel, M., Leroy, J.L. (Eds.), Source, Transport and Deposition of Metals. Balkema, Rotterdam, 325–328.

Luiders, V., Gerler, J., Hein, U. F. and Reutel, Chr. (1993): Chemical and thermal developments of ore-forming solutions in the Harz Mountains: a summary of fluid inclusion studies. Monogr. Ser. Miner. Deposits, 30, 117-132.

Mackenzie, K. J. D. and Green, J. M. (1971): The cause of colouration in Derbyshire blue john banded fluorite and other blue banded fluorite. Mineral Magz., 38, 459-70.

Mahdy, N. M., Shalaby, M. H., Helmy, H. M., Osman, A. F., El Sawy, E. and Abu Zeid E. K. (2013): Trace and REE element geochemistry of fluorite and its relation to uranium mineralizations, gabal gattar area, northern eastern Desert. Egypt. Arab. J. Geosci. 7 (7), 2573-2589.

Maurice, A. E., Bakhit, B. R., Basta, F. F. and Khiamy, A. A. (2013): Geochemistry of gabbros and granitoids (M- and I-types) from the Nubian Shield of Egypt: roots of Neoproterozoic intra-oceanic island arc. Precamb. Res., 224, 397–411.

Michard, A. (1989): Rare earth element systematics in hydrothermal fluids. Geochim. Cosmochim. Acta 53, 745–750.

Mohamed, N. A. (1995): Distribution and extraction of uranium and some trace elements from the mineralized zones of EL-Missikat – EL-Erediya area, Eastern Desert, Egypt. Ph.D. Thesis, Fa-culty of Science, Cairo Univ., 1-185.

Mohamed, M. A. (2013): Evolution of mineralizing fluids of cassiteriteewolframite and fluorite deposits from Mueilha tin mine area, Eastern Desert of Egypt, evidence from fluid inclusion. Arab. J. Geosci. 6, 775-782.

Mohamed, M. A. and Bishara, W. W. (1998): Fluid inclusions study of Sn-Wmineralization at Igla area central Eastern Desert. Egypt. Geol. Soc. Egypt Cairo 42 (1), 207-220.

Moldovanyi, E.P. and Walter, L.M. (1992): Regional trends in water chemistry, Smackover Formation, Southwest Arkansas; geochemical and physical controls. The American Association of Petroleum Geologists Bulletin 76 (6), 864–894.

Möller P, Bau M, Dulski P and Luders V. (1998): REE and yttrium fractionation in fluorite and their bearing on fluorite formation. Proc 9th Quadr IAGOD Symp., 575-592.

Möller P and Holzbercher E. (1998): Eu anomalies in hydrothermal fluids and minerals. A combined thermochemical and dynamic phenomenon. Freib Forsch hefte 475, 73-84.

Möller, P. and Morteani, G. (1983): On the geochemical fractionation of rare earth elements during the formation of Ca-minerals and its application to problems of the genesis of ore deposits. In: Augustithis, S.S. (Ed.), The Significance of Trace Elements in Solving Petrogenetic Problems and Controversies. Theophrastus, Athens, 747-791.

Möller, P., Parekh, P. P. and Schneider, H. J. (1976): The application of Tb/Ca-Tb/La abundance ratios to problems of fluorspar genesis. Mineralium Deposita 11, 11-l16.

Mollow, E. (1934): Electron conduction and colour centres in fluorspar. Nachrichten von der Gesellschafdt er lltissenschaften zu Goettingen, Fachgruppe, 2, 79-89.

Nachit, H., Ibhi, A., Abia, E. H. and Ohoud, M. B. (2005): Discrimination between primary magmatic biotites, reequilibrated biotites and neoformed biotites. Comptes Rendus Géoscience 337, 1415-1420.

Nachit, H., Razafimahefa, N., Stussi, J.M. and Carron, J.P. (1985): Composition chimique des biotites et typologie magmatique des granitoides. Comptes Rendus Hebdomadaires de l" Academie des sciences 301(11), 813-818.

Nockolds, S.R. (1947): The relation between chemical composition and petrogenesis in biotites of micas of igneous rocks. J. Sci., 245 (5), 401-420.

Oliver, N.H.S., McLellan, J.G., Hobbs, B.E., Cleverley, J.S., Ord, A. and Feltrin, L. (2006): Numerical models of extensional deformation, heat transfer, and fluid flow across basement cover interfaces during basin-relatedmineralization. Econ. Geol., 101 (1), 1–31.

Patino Douce, A. E. (1993): Titanium substitution in biotite: an empirical model with applications to thermometry, O_2 and H_2O barometries, and consequences form biotite stability. Chem. Geol., 108, 133-162.

Piqué À., Canals, A., Grandia, F., David A. and Banks, D.A. (2008): Mesozoic fluorite veins in NE Spain record regional base metal-rich brine circulation through basin and basement during extensional events. Chem. Geol., 257, 139–152.

Pirajno, F. (2009): Hydrothermal Processes and Mineral Systems. Geol. Surv. Western Australia. Springer.

Pitcher, W. S. (1997): The Nature and Origin of Granite, 2nd ed., London: Chapman & Hall, 386.

Przibram, K. (1956): Irradiation colour and luminescence: Pergamon Press London, 216p.

Raslan, M. F. (2008): Beneficiation of uranium-rich fluorite from El-Missikat mineralized granite, Central Eastern Desert, Egypt, Physicochemical Problems of Mineral Processing Journal, 42, 185-194.

Raslan, M. F. (2009): Mineralogical and geochemical characteristics of uranium-rich fluorite in El-Missikat mineralized granite, Central Eastern Desert, Egypt. Geologija. 52/2, 213-220

Rasmy, M., Guirguis, L.A. and Bakhit, F.S. (1992): Occurrnce and geochemistry of some fluorite veins in the central part of the Eastern Desert. Proc. Egypt. Acad. Sci.

Rieder, M., Cavazzini, G., D'yakonov, Y. S., Frank-Kamenetskii, V. A., Gottardi, G., Guggenheim, S., Koval', P. V., Müller, G., Neiva, A. M. R., Radoslovich, E. W., Robert, J.-L., Sassi, F. P., Takeda, H., Weiss, Z. and Wones, D.R. (1998): Nomenclature of micas. Canadian Mineralogist 36, 905-912.

Robb, L. J. (2005): Introduction to Ore-forming Processes. Blackwell Science Ltd, p. 386

Roedder, E. (1984): Fluid inclusions. Mineral. Soc. Amer. 12. In: Ribbe, P.H. (Ed.), Reviews in Mineralogy, p. 644.

Roedder, E. and Bodnar, E. (1997): Fluid inclusion studies of hydrothermal ore deposits. In: Barnes, H.L. (Ed.), Geochemistry of Hydrothermal Ore Deposits. John Wiley &Sons, Inc., p. 972.

Russo R. E., Mao X., Liu H., Gonzalez J. and Samuel S. M. (2002): Laser ablation in analytical chemistry—a review. Talanta, 57, 425-451.

Sabet, A. H., Tsoggoev, VOL. B., Spiridonov, VOL. P., Sarin, L. P. and Abdel Nabi, a. a. (1976): Geologic structure and laws of localization of tin-beryllium mineralization at Igla deposits. Annals Geol. Surv. Egypt. 6, 175-168.

Salem, I. A., Abdel-Moneim, A. A., Shazly, A. G., El-Shibiny, N. H., (2001): Mineralogy and geochemistry of Gabal El-lneigi Granite and associated fluorite veins, Central Eastern Desert, Egypt: application of fluid inclusions to fluorite genesis. J. Afr. Earth Sci. 32 (1), 29-45.

Schwinn, G. and Markl, G. (2005). REE systematics in hydrothermal fluorite. Chem Geol 216, 225–248.

Serra, A. (1947): Osservazion: Specttroscpiche su fluorine Colarate-Ricerca Sci.Ricostr. Roma, 17, 670.

Schönenbeger, J., Köhler, J. and Markl, G. (2008): REE systematic of fluorides, calcite and siderite in perkaline plutonic rocks from the Gardar Province, South Greenland. Chem. Geol., 247, 16-35.

Shelton, K.L., Burstein, I.B., Hagni, R.D., Vierrether, C.B., Grant, S.K., Hennigh, Q.T., Bradley, M.F. and Brandom, R.T. (1995): Sulfur isotope evidence for penetration of MVT fluids into igneous basement rocks, southeast Missouri, USA. Mineralium Deposita, 30 (5), 339-350.

Shunda Y., Jiantang1 P., Ruizhong H., Xianwu B., Liang Q., Zhaoli L., Xiaomin L. and Yan, S. (2008): Characteristics of rare-earth elements (REE), strontium and neodymium isotopes in hydrothermal fluorites from the Bailashui tin deposit in the Furong ore field, southern Hunan Province, China. Chin.J.Geochem 27, 342-350.

Sierro, J. (1963): RPE de Gd^{+3} dans CaF_2, BaF_2, SrF_2, He1v. Phys. Act. 36, p.505.

Sylvester, P. J. (1989): Post-collisional alkaline granites, J. Geol., 97, 261-280.

Wassef, B. and Kamel, O.A., et al. (1973): Report on the results of the prospecting work for gold in El Sid-Semna area in 1970/1971. Geol. Surv. Egypt, internal report no. 23/1973.

Whalen, J. B., Currie, K. L. and Chappel, B. W. (1987): A-type granites: geochemical characteristics, discrimination and petrogenesis, Cont. Min. Pet., 95: 407―19.

Whalen, J. B., Jenner, G. A. and Longstaffe, F. J. et al. (1996): Geochemical and isotopic (O, Nd, Pb and Sr) constraints on A-type granite: petrogenesis based on the Topsails igneous suite, Newfoundland Appalachians, J. Petrol., 37, 1463-1489.

Wilkinson, J. J. (2001): Fluid inclusions in hydrothermal ore deposits, Lithos. 55, 229-272

Wood, S.A. (1990): The aqueous geochemistry of the rare-earth elements and yttrium. 1. Review of available low-temperature data for inorganic complexes and inorganic REE speciation of natural waters. Chem. Geol., 82, 159-186.

Worden, R.H., Manning, D.A.C. and Bottrell, S.H. (2006): Multiple generations of high salinity formation water in the Triassic Sherwood Sandstone: Wytch Farm oilfield, onshore UK. Appl. Geochem. 21 (3), 455–475.

Yonan, A.A. (1990): Mineralogical, Petrochemical and Geochemical Studies on Granites Hosting Fluorite Mineralizations in the Eastern Desert of Egypt. Unpubl. Ph.D. Thesis. Geol. Dept., Fac. Sci., Ain Shams Univ., Egypt.

Yonan, A. A. and El-Kammar, A. (2001): Implications of Y-HREES geochemistry in interpreting genesis of fluorite from magmatic-hydrothermal system: Acase study from Egypt. Egypt. J. Geol., 45(2), 941-951.

Zak, K., Cadek, J., Dobes, P., Smejkal, V., Reichmann, F., Vokurka, K. and Sandstat, J.S. (1990): Vein barite mineralization of the Bohemian massif: sulfur, oxygen and strontium isotopes and fluid inclusion characteristics and their genetic implications. In: F.G. Poole and P. Dobes (Editors), Pm. Symp. on Barite and Barite Deposits, Kutna Hora, Sept. 20-23, 1988, 35-49.

الخصائص المعدنية والجيوكيميائية لتمعدن الفلوريت بالميسيكات ، بوسط الصحراء الشرقية ، مصر : مقصورة على العناصر الشحيحة ومكتنفات المائع

بطرس رياض بخيت

قسم الجيولوجيا –كلية العلوم – جامعة بنى سويف

الخلاصة

يتواجد الفلوريت بمنطقة الميسيكات كعروق رقيقة وحبيبات متناثرة فى الجرانيت المضيف . ويتناول البحث الخصائص المعدنية و الجيوكيميائية، بما في ذلك كيمياء المعادن وتحاليل العناصر الأساسية والشحيحة وعناصر REY (العناصر الأرضية النادرة والايتريوم) لصخر الجرانيت المضيف للفلوريت. بالإضافة الى القياسات المختلفة للمكتنفات السائلة الاولية الموجودة فى الفلوريت ولقد تم تحليلها (لاول مرة فى مصر) باستخدام جهاز (LA–ICP–MS) .

أوضحت الدراسات الميكروسكوبية ان الصخر المضيف ممثل بالجرانيت البيوتايتى. كما أوضحت نتائج الميكروبروب بان البيوتيت هو أولي من أصل نارى وتبلور في ٥٠٠ الى ٦٠٠°م . وجيوكيميائيا الجرانيت المضيف هو من النوع القلوى (A–Type) وتكون في بيئة ما بعد الاصطدام .

يتزايد متوسط محتوى العناصر الأرضية النادرة (ΣREE) للفلوريت البنفسجي (نوعV) من ٧٥.٥ جزء فى المليون الى ٢٠٠.٩ و٢٠٣.٢ جزء في المليون للفلوريت الأخضر (نوع G) والفلوريت الابيض (نوع W) على التوالي وهذه الاختلافات في ΣREE ربما ترتبط بالتغيرات في حالة الحموضة (pH) والتركيب الكيميائي الكلى للمائع .

وأوضحت الدراسة إن الفلوريت تشكل من التفاعل بين السوائل المنصهرة و الجرانيت المضيف ويتميز الفلوريت بافتقارة الشديد للايربيوم (Eu) وغنى شديد لعنصر الاتريوم (Y) ومشابها بذلك لنمط العناصر الأرضية النادرة للجرانيت المضيف ، مشيرا إلى أن مصدر العناصر الأرضية النادرة هو الجرانيت وتم سحبها بواسطة السوائل الحرارية المائية.

وكشفت الدراسة الحالية أن غنى الإتريوم ومجموع محتويات العناصر الأرضية النادرة هي المسئولة عن ظهور اللون الأخضر والأبيض للفلوريت ، واما المحتوى العالي للاسترنشيوم في الفلوريت البنفسجي قد تكون المسئول عن اللون البنفسجي للفلوريت.

واوضحت دراسة مكتنفات الموائع أن درجات حرارة التجانس تتراوح بين ٢٠١°م إلى ٢٩٦°م في السوائل مرتفعة الملوحة (Type A FI) و ١٦٠°م إلى ١٦٥°م في السوائل منخفضة الملوحة (Type B FI). وتشير الدراسة ان نسبة الملوحة تصل إلى ١٩.٤ وزن مكافئ ٪ فى النوع الاول (Type A FI) و ٠.٥٣الى ٤.٤٩ فى سوائل النوع الثانى (Type B) . وكثافة السوائل هي ٠.٩الى ١.٠ جم/ سم^3 في نوع A و ٠.٩ جم/ سم^3 في النوع B.

واوضحت تحاليل مكتنفات الموائع بواسطة جهاز LA–ICP–MS تركيزات العناصر المختلفة فى السوائل المسببة لتمعدن الفلوريت وقد وجد ان النوع العالى الملوحة (Type A FI) يحتوي على تركيزات عالية جدا من معظم العناصر مقارنة بالنوع المنخفض الملوحة وهو المصدر الاساسى للعناصر فى الفلوريت . وآليات ترسب الفلوريت قد يكون خلط السوائل معا والتغيرات في الضغط ودرجة الحرارة بالإضافة الى تفاعل السوائل والصخور المضيفة.